4 Transcription profiling of murine ES cells infected by *S.* Typhimurium SL1344

4.1 Introduction

4.1.1 Microarrays in host-pathogen interactions studies

Microarray analysis was introduced in the mid-1990s and since then this approach has been the method of choice for large-scale gene expression studies. Microarrays provide an efficient and rapid method to investigate the entire transcriptome of a cell or cell population. Perhaps no research field has benefited more from microarray technology than the study of the interplay between pathogens and their hosts (McGuire & Glass, 2005). Figure 4.1 summarize examples of the applications that microarrays can have in infectious diseases and host-pathogen interactions studies (Bryant *et al.*, 2004). The expansion of this technology takes advantage of the recent escalation in DNA sequence resources. In fact the complete genome of a large number of pathogens has now been fully sequenced in addition to the human and mouse genomes, permitting an exhaustive investigation of host-pathogen interactions.

Host-pathogen interactions can be investigated from either the perspective of the host or from that of the pathogen. Microarrays have been designed for a large range of pathogens including *Escherichia coli*, *Leishmania* species, *Bordetella pertussis*, *Yersinia pestis* and *S.* Typhimurium (McGuire & Glass, 2005). Even without the whole genome level of sequence knowledge, shotgun microarrays can be constructed from genomic DNA libraries (Hayward *et al.*, 2000b). One intriguing feature of pathogen microarray studies is the differential expression patterns observed in a large number of genes with no known function. This is the case even in the extensively genetically mapped bacteria *S.* Typhimurium where the function of many genes has been determined. *S.* Typhimurium has been the subject of expression profile studies looking at the bacterial SCV transcriptome profile during infection of macrophages (Clements *et al.*, 2002; Eriksson *et al.*, 2003).

Microarray studies performed on host RNA responses have exploited a variety of *in vivo* and *in vitro* models of human, mouse and other species. These studies can now exploit commercial species-specific arrays such as the Affymetrix porcine GeneChip, specific for pig. A few groups have conducted investigations on the host response to *Salmonella*, both on *ex-vivo* tissues or on *in vitro* models. One of the first reports to be published was in 2000 by Rosenberger *et al.*, who reported changes in gene expression in mouse macrophages during *S.* Typhimurium infection and the effects of LPS as a bacterial virulence factor (Rosenberger *et al.*, 2000). In this study Atlas mouse cDNA expression arrays were employed. These arrays contained duplicate spots of 588 mouse partial cDNAs. Murine macrophages RAW 264.7 were infected with *S.* Typhimurium SL1344 or stimulated with 100ng/ml of LPS, and at 4 hours post infection (pi) total RNA was isolated. At 4 hours post-infection the expression levels of 77 out of 588 genes represented on the array were detectably altered by two-fold or more in the RAW 264.7 macrophages. Among the up-regulated genes were LIF, CD40, IL-1β, ICAM-1, TGF β2, MIP-1(α, β and 2α) and iNOS, and among the down-regulated genes were the IL-6 receptor and a few cyclins. Many of these genes are involved in the immune response. Also a number of transcription factors were regulated by *S.* Typhimurium infection; Egr-1, NF-E2, IRF-1 and c-rel were induced whereas Ski, B-myb, Fli-1 and c-Fes were suppressed. This study highlighted a remarkable overlap of genes induced by *S.* Typhimurium and purified *S.* Typhimurium LPS suggesting a 'redundancy' in host response to bacteria and some of their products (Rosenberger *et al.*, 2000).

In a second study on the *in vitro* host response to *S.* Typhimurium, Detweiler *et al.* investigated the response of U-937 human macrophages to wild-type SL1344 and a *phoP* mutant using an in-house human spotted array with 22,571 cDNA. This study reported 68 genes with a two-fold or greater difference in expression level between uninfected and infected macrophages. Among the genes reported to be induced were IL-8, MIP-1α and β, IL1β, IL-23p19, NF-κB and a several transcription factors. However they did not present any data on genes that were down regulated, although genes that were unregulated in the cells infected with the wild-type compared to the *phoP* mutant bacteria were included. Among these genes were CD9, cathepsin D, SSI-3 and contactin 1. The *phoP::Tn10* mutant strain elicited many of the same mRNA transcripts as the wild-type bacteria and overall the inflammatory response in U-937 macrophages to

wild-type *Salmonella* and the *phoP::Tn10* mutant strain were similar. Nevertheless, this report identified 34 mRNAs with expression levels 1.9 times lower in *phoP::Tn10* infected macrophages than in wild-type infected macrophages. Of these about a third of the twenty-one with known function were involved in cell death. In this study, microarray analysis provided a tool to identify host molecular pathways influenced by a virulence determinant (Detweiler *et al.*, 2001). In fact as a long-term survival strategy, pathogens can alter host gene transcription to maintain a hospitable niche and prevent detection and clearance by the immune system (Rosenberger *et al.*, 2001).

In another study conducted in 2002, Nau *et al*. investigated the macrophage response to different bacterial pathogens in the hope of improving our understanding of host defenses and discovering the theme that defines the innate immune responses of the macrophage to bacteria (Nau *et al.*, 2002). With this purpose in mind they infected human monocytes with *Staphylococcus aureus* strain ISP794, *Listeria monocytogenes* strain EGD, *Mycobacterium tuberculosis* Erdam strain, *M. bovis* BCG, *S.* Typhi Quailes strain, *S.* Typhimurium (ATCC no. 14028), *E. coli* strain sd-4, and enterohaemorrhagic *E. coli* O157:H7. Human macrophages derived from primary monocytes were exposed to bacteria and bacterial components and the resulting expression levels of 6,800 genes were monitored over 24 hours. The researchers were able to highlight a common core of genes differentially expressed during the infection of all the bacteria: 132 genes were induced and 59 genes were suppressed. The up-regulated genes were listed in the following categories: cytokines, chemokine, proliferation, tissue remodelling, adhesion, receptors, transcription, transporters, enzymes, pro-inflammatory, anti-apoptotic, stress response and signaling; the down-regulated genes were organized in the categories: anti-inflammatory, pro-inflammatory, adhesion, receptors, signaling, transcription, transporters, tissue remodelling, and enzymes (Nau *et al.*, 2002).

These studies were conducted on macrophages but *Salmonella* is also able to invade epithelial cells and in 2000, Eckmann *et al*. reported the response of human HT-29 colorectal epithelial cells and T84 human colon epithelial cells to *S. dublin*. In their studies they utilised two different cDNA arrays: GF211 Human "Named genes" GeneFiltered Release I from Research Genetics Inc. (Huntsville, AL) and the Atlas Cytokine/Receptor cDNA Expression Array from CLONTECH Laboratories (PaloAlto, CA) (Eckmann *et al.*, 2000). In the first experiments they employed the GF211 array

(which incorporated 4000 human cDNAs). They analysed mRNA extracted from epithelial cells at 3, 8 and 20 hours, post-infection and reported that the vast majority of the genes (~95%) showed relatively little change. They postulated that the up-regulated genes may be more important than those down-regulated so they concentrated their attention on the former. Among the genes differentially expressed at 3 hours infection were IL-12p40, IL-8 and MHC Class I heavy chain, LI-cadherin and ubiquitin-conjugating enzyme E2. Subsequently, they investigated the RNA expression profile of similar epithelial cells during *S. dublin* infection using the Atlas Human Cytokines/Receptor array (CLONTECH) (with 277 cDNAs from cytokines and receptors). They reported the top 25 differentially expressed genes, which included ubiquitin, LIF, insulin receptor along with IL-8, IL-17 and G-CSF (Eckmann *et al.*, 2000).

It is somewhat surprising that cyclins were not differentially expressed in this study because others have reported differences in similar assays (Nau *et al.*, 2002). Possibly, these researchers were very much interested in looking at the immune response and not at the events at the cellular level in reaction to the pathogen. It can be concluded from these studies that many variables are potentially present in this type of research (cell type, pathogen type, time of infection, type of array platform and data analysis methods) and they can influence the outcome of the analysis and the subsequent conclusions. These studies also reveal the complexity of the models employed. Perhaps it might be useful to interpret host-pathogen interactions on three levels: immunological response, usually predominant; the pathogen orchestration of the host genome, that is not very easy to discern; and the cellular reaction to invasion.

The experimental results reported in Chapter 3 suggested that mouse ES cells could be a promising model to study host-pathogen interactions and to further confirm this hypotesis experiments were performed to explore ES cell mRNA expression profiles during bacterial infection by microarray analysis. These data could advance the understanding of mouse ES cell gene regulation and other characteristics in addition to providing insight into host-pathogen interactions. The results from microarray expression profiling of AB2.2 murine embryonic stem (ES) cells infected with *S.* Typhimurium SL1344 at 2 and 4 hours are reported in this chapter. The rational for these studies was to provide insight into the response of ES cells to pathogen invasion,

helping us to understand how this new *in vitro* model compares to those previously characterized. This is part of the planned investigation of the feasibility of using murine ES cells to study infectious diseases. It is hoped that the results obtained here will help to direct future investigations involving genetically mutated ES cells or differentiated cells.

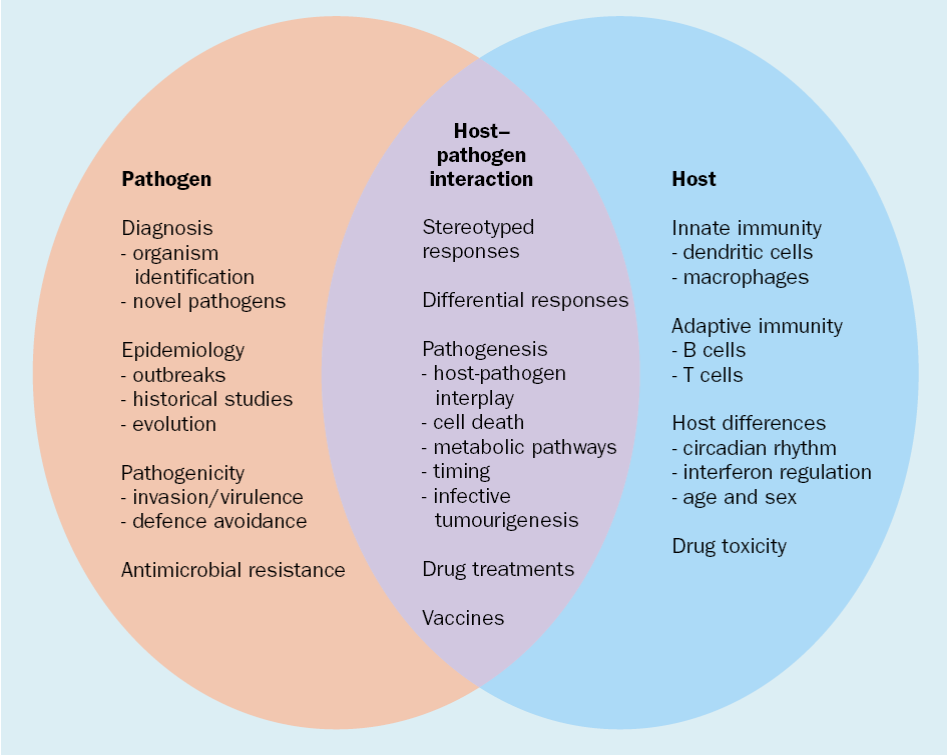

Figure 4.1 Host-pathogen interactions that can be exploited using microarray technology
Microarray technology has a great potential in infectious disease research, helping to explore the complex interactions between host and pathogen and reveal new routes for treatments (Bryant et al., 2004).

4.2 Experimental design

Three independent biological replicates of AB2.2 murine ES cells were infected for 2 hours and 4 hours with *S.* Typhimurium SL1344. Each biological replicate was treated in the same way and total RNA was extracted at time zero from uninfected cells and at 2 hours and 4 hours infection after 30 minutes incubation with the bacterial suspension. Samples of the cells infected at each time point were analyzed by FACS in order to establish the percentage of infected cells. For this reason *S.* Typhimurium SL1344 (p1C/1) expressing GFP was used in these experiments. Three time points (0h, 2h, 4h) were chosen for each of the three biological replicates, giving a total of nine RNA samples for analysis. Also, for each time point three technical replicates were performed for a total of 27 arrays. For each technical replicate an independent cDNA synthesis and cRNA labelling was performed and analyzed by Agilent Bioanalyzer before being hybridized on Affymetrix GenChip® Mouse 430.20 arrays (Affymetrix, 2004). The expression data were then analyzed using three different packages: Bioconductor and GeneSpring were used to compare the gene expression profile at 2h and 4h infection to the uninfected cells' mRNA profile and between each other; and ANOVA Simultaneous Component Analysis (ASCA) platform was used to carry out a time course analysis where the time was counted as a variable.

4.3 Results

4.3.1 Murine ES cell infection with *S.* Typhimurium and total RNA extraction

AB2.2 mouse ES cells were maintained undifferentiated in culture media with 1000U/ml of LIF, at 37ºC and 5% CO_2. The cells were seeded at $2.5x10^5$ cells per well in 6-well plates and grown for 2 days until 90% confluent. *S.* Typhimurium(p1C/1) expressing GFP was used in these experiments in order to perform parallel flow cytometric examination of the percent of infected cells. *Salmonella* was grown as described in M&M and was seeded into cell culture at MOI ~ 100. After 30 minutes incubation at 37ºC the cells were washed with warm Dulbecco's PBS Ca^-Mg^- and incubated for 2 hours or 4 hours with complete DMEM medium containing 50μg/ml of gentamicin antibiotic. The cells were then washed and the cells from three wells were trypsinized and analyzed by FACS, whereas the cells in the other three wells were scraped and frozen at -80ºC.

Only those cells in which the infection rate was above 30%, as determined by cytometric analysis, were further used for total RNA extraction with the QIAGEN RNeasy Midi kit. The first biological replicate of AB2.2 murine ES cells (passage 33) was infected with *S.* Typhimurium and it was established by flow cytometric analysis that at 2 hours and 4 hours, 30% and 32% of the cells were infected respectively. In the second biological replicate AB2.2 murine ES cells were infected at passage 27 and flow cytometric analysis established that at 2 hours and 4 hours, 42% and 36% of the cells were infected respectively. The third replicate AB2.2 murine ES cells were infected at passage 26 and at 2 hours and 4 hours, 34% and 30% of the cells were infected respectively. An example of the FACS analysis of these cells can be found in Figure 4.2.

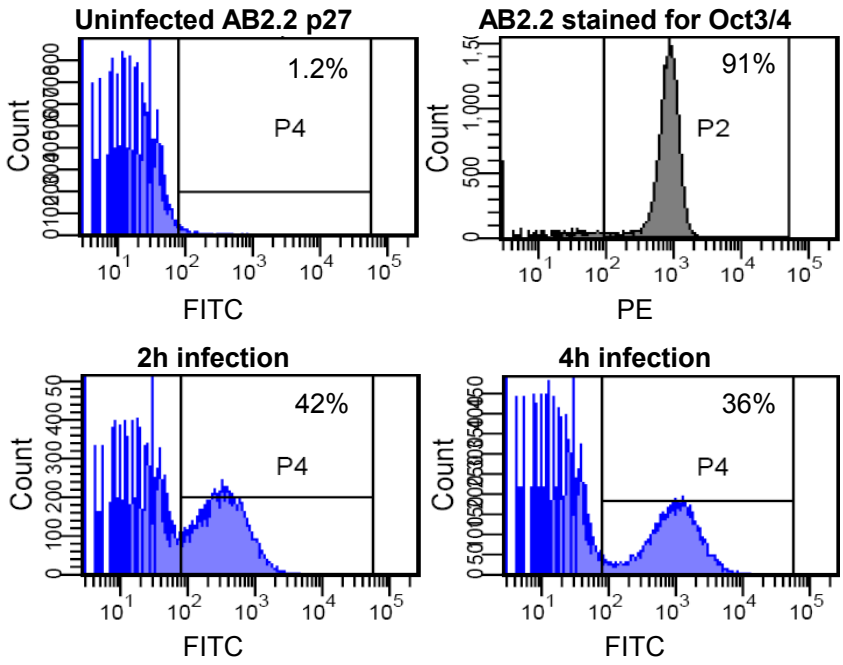

Figure 4.2 Flow cytometric analysis of murine ES cells infected with *S.* Typhimurium SL1344

The AB2.2 murine ES cells were analyzed in parallel by FACS in order to investigate the percentage of infected cells prior to RNA extraction. For this reason *S.* Typhimurium(pC1/1) expressing GFP protein was used for these experiments. In addition Oct3/4 analysis was performed on uninfected cells in order to confirm their pluripotency characteristic.

4.3.2 Murine ES cell total RNA extraction and analysis

The total RNA was extracted using the QIAGEN RNeasy Midi Kit following the manufacturer's instructions. The concentration of total RNA extracted was measured using the NanoDrop1000 (Thermo) spectrophotometer. NanoDrop1000 is a full-spectrum UV/Visible (220-750nm) spectrophotometer used to quantify nucleic acids in a small volume as little as 1µl. The technology used exploits surface tension of small volumes [www.nanodrop.com]. The final concentrations obtained for each sample are reported in Table 4.1.

Table 4.1 Total RNA concentration of murine ES cells infected by *S.* Typhimurium(p1C/1) measured with NanoDrop1000 technology

Sample ID	Description	ng/µl	260/280 Ratio
1	AB2.2 First Biological Replicate	718	2.12
2	AB2.2 First Biological Replicate Infected with SL1344/p1C/1 2h	642	2.12
3	AB2.2 First Biological Replicate Infected with SL1344/p1C/1 4h	830	2.12
4	AB2.2 Second Biological Replicate	914	2.12
5	AB2.2 Second Biological Replicate Infected with SL1344/p1C/1 2h	792	2.12
6	AB2.2 Second Biological Replicate Infected with SL1344/p1C/1 4h	855	2.13
7	AB2.2 Third Biological Replicate	909	2.12
8	AB2.2 Third Biological Replicate Infected with SL1344/p1C/1 2h	707	2.04
9	AB2.2 Third Biological Replicate Infected with SL1344/p1C/1 4h	892	2.12

To test the RNA quality, the samples were analyzed using the Agilent 2100 Bioanalyzer (Agilent Technologies, Palo Alto, CA, USA). The Bioanalyzer is an automated bio-analytical device using microfluidics technology that provides electrophoretic separation in an automated and reproducible manner (Schroeder *et al.*, 2006). Bioanalyzer was used in this study to evaluate the quality of the total RNA extracted from mouse ES cells uninfected and infected by *S.* Typhimurium. Figure 4.3 reports an example of the quality of the total RNA obtained from AB2.2 murine ES cells uninfected and infected at 2 hours and 4 hours with *S.* Typhimurium SL1344(p1C/1).

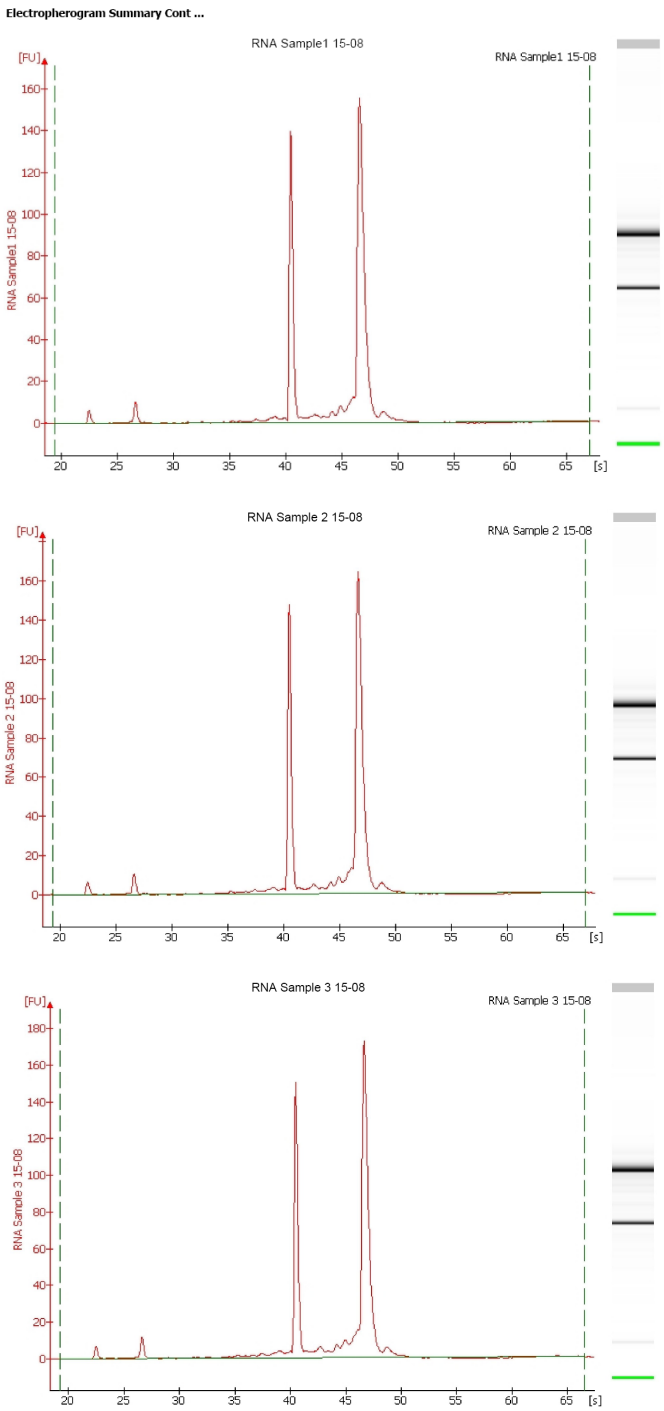

Figure 4.3 Bioanalyzer analysis of total RNA from infected and uninfected ES cells

The quality of the total RNA extracted from each sample was analyzed by Bioanalyzer before microarray analysis.. Representative histograms of the RNA quality from AB2.2 murine ES cells uninfected (top) or infected with *S.* Typhimurium SL1344(p1C/1) at the 2h (middle) and 4h invasion (bottom histogram) with the respective virtual gel, are represented. The histograms reveal two peaks representing the ribosomal RNA 18S and the 28S, from the left. The intensity of the gel band of 28S ribosomal RNA should be about twice that of the 18S ribosomal band.

4.3.3 cRNA synthesis, labelling and microarray hybridization

In order to analyze the expression profile of murine ES cells, the total RNA extracted was hybridized on the Affymetrix GeneChip® Mouse 430 2.0 Array following the manufacturer's instructions. Briefly, the 5µg of total RNA was used to synthesize double stranded cDNA using the One-Cycle cDNA Synthesis Kit which use poly-T primers. This was 'cleaned' from traces of RNA and used as template for the synthesis of Biotin-Labeled cRNA with the One-cycle Target Labelling Assay kit, following the manufacturer's directions. Then cRNA was cleaned and quantified and its quality was analyzed by Bioanalyzer before hybridization (Figure 4.4). An independent cDNA synthesis and cRNA labelling reaction was carried out for each technical replicate. The cRNA was first fragmented before hybridization and 15µg of cRNA per chip was used for hybridization at 45ºC in constant rotation (60 rpm) overnight. The chips were washed and scanned at the Fluidics Station 450 operated using GCOS/Microarray Suite software.

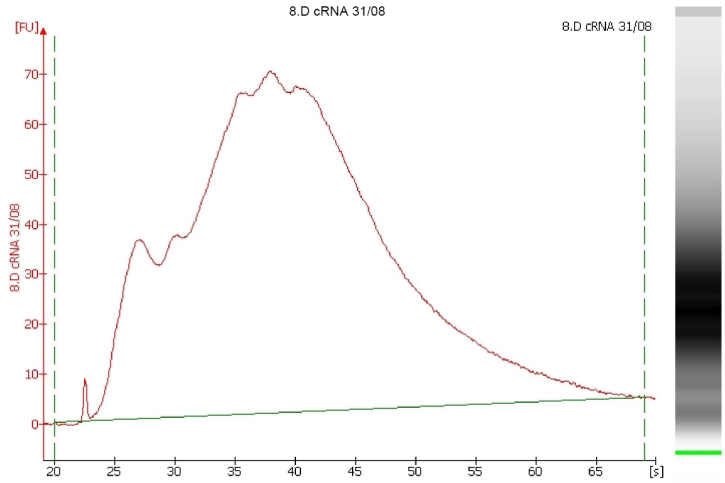

Figure 4.4 Bioanalyzer analysis of the biotin-labelled cRNA

As the Affymetrix manual reports, the cRNA quality needs to be confirmed by Bioanalyzer to prove that the cRNA amplification reaction worked. The optimum is to obtain cRNA fragments between 500-1500 nucleotides, which corresponds to 35 and 40 seconds, respectively. This picture reports an example of the cRNA obtained in this study.

The Affymetrix GeneChip® Mouse Genome 430 2.0 Array used harbours 45,000 probes representing transcripts and variants from over 34,000 well characterized mouse genes (Affymetrix, 2004). The Affymetrix expression array uses a set of features (spots), each designed to recognize a molecule of interest. Each feature consists of millions of identical single-stranded 25-mer nucleotide probes designed to hybridize to a specific transcript. The probes are defined Perfect-Match (PM) features and each is accompanied by an adjacent Mis-Match (MM) feature in which the middle residue is changed. Hybridization conditions are designed to maximize binding to the PM feature while minimizing binding to the MM ones. The MM signal can be used to provide a measure of probe specific background for its PM partner. Multiple PM/MM pairs are used for each transcript (Okoniewski & Miller, 2008).

4.3.4 Microarray data analysis

4.3.4.1 Bioconductor analysis

4.3.4.1.1 Results from Bioconductor pair-comparison analysis

Microarray expression profile analysis was initially conducted using Bioconductor [Bioconductor: http://www.bioconductor.org] (Gentleman *et al.*, 2004). Bioconductor is a collection of open source software packages designed to support the analysis of biological data. Bioconductor is written using the programming language R, which itself provides access to a wide range of tools for statistical analysis, data presentation, and visualization (Okoniewski & Miller, 2008). In this analysis the mouse ES cell microarray profiles at 2 hours and 4 hours post-infection were compared with the profile of uninfected cells (0h). The arrays were first subjected to quality control and the report can be seen in Appendix A. Normalization using GCRMA (Wu *et al.*, 2004) was then performed and this includes background adjustment, quantile normalization, and median-polish summarization at the probe level. The data were then further analyzed using the Limma package and applying a linear model to estimate the effect of each factor on the variance of the data [limma : http://bioinf.wehi.edu.au/limma/]. The results from this analysis are reported in Tables 4.2, 4.3 and 4.4

Table 4.2 Bioconductor analysis of RNA expression profile of murine ES cells at 2h infection

The mRNA expression profile of uninfected AB2.2 murine ES cells and that obtained following 2h infection with *S.* Typhimurium were compared and analyzed using the Bioconductor package; significantly differentially expressed genes are reported (p-value <0.05 and fold change +/- 1.5).

Fold Change	Adj.p-value	Gene Symbol	Gene Title	Process and Functions
10.63	0.0007	Cyp1b1	cytochrome P450, family 1, subfamily b, polypeptide 1	oxidation reduction// monooxygenease activity// iron ion binding// electron carrier activity// ER membrane
4.38	0.0147	Cyp1a1	cytochrome P450, family 1, subfamily a, polypeptide 1	dibenzo-p-dioxin metabolic process // oxidation reduction// monooxygenease activity// iron ion binding// ER membrane

Table 4.3 Bioconductor analysis of RNA expression profile of murine ES cells at 4h infection

Genes determined to be differentially expressed following Bioconductor analysis of arrays hybridized with mRNA from uninfected AB2.2 ES cells and infected with *S.* Typhimurium for 4h. The 30 genes reported are significantly differentially expressed at 4h infection compared to uninfected cells (0h) (p value < 0.05 and fold change +/- 1.5; * = gene reported twice; ** = gene reported three times)

Fold Change	Adj. p value	Gene symbol	Gene Name	Process and Functions
2.32	0.0327	Banp	Btg3 associated nuclear protein	Transcription/ cell cycle/ DNA binding
2.25	0.0002	Hspa1b**	Heat shock protein1B	DNA repair//anti-apoptotic//response to stress
2.01	0.0053	Pdxp	Pyridoxal (vitB6) phosphatase	Magnesium ion binding//catalytic activity
2	0.0065	Zbtb40	Zinc finger and BTB domain containing 40	Nucleic acid binding//zinc binding// prot. binding
1.88	0.0464	Ccng2	Cyclin G2	Cyclin-dependent protein kinase regulator activity
1.84	0.002	Herpud1	Homocystein-inducible, ER stress-inducible, ubiquitin-like domain member 1	Response to stress// response to unfolded protein
1.64	0.0011	Tbl2	Transducin(beta)-like 2	//
1.62	0.0211	Ankrd37	Ankyrin repeat domain 37	//
1.6	0.0336	Aof1	Amine oxidase, flavin containing 1	Zinc binging // electron carrier activity
1.55	0.0016	Clk2	CDC-like kinase 2	Nucleotide binding// protein kinase activity// ATP binding
1.55	0.017	Pex11a	Peroxisomal biogenesis factor 11a	Peroxisome organization and biogenesis
1.54	0.0125	Ccdc117	Coiled-coil domain containing 117	//
1.53	0.0049	Luc7l	Luc7 homolog (*S. cerevisiae*)-like	Zinc ion binding// metal ion binding
1.53	0.017	Xbp1	X-box binding protein 1	Transcription factor activity
1.51	0.0334	C430002E04Rik	RIKEN cDNA C430002E04 gene	//
-1.51	0	Sfrs5	Splicing factor arginine/serine-rich 5 (SRp40, HRS)	Nucleic acid binding
-1.52	0.0336	LOC100044766	Similar tow domain-containing adapter protein with coiled-coil	Protein binding
-1.55	0.0334	Msc	Musculin	Transcription regulator activity
-1.55	0.0052	Chic2	Cycteine-rish hydrophobic domain 2	Golgi to plasma membrane transport
-1.57	0.0129	1810013L24Rik	RIKEN cDNA 1819913L24gene	//
-1.65	0.0039	Lrpap1*	Low density lipoprotein receptor-related protein associated protein 1	Receptor activity// low-density lipoprotein receptor binding
-1.65	0.0084	Slc7a1	Soluble carrier family 7 member 1	Receptor activity// amino acid transmembrane transporter activity
-1.78	0.0001	LOC100046855	Similar to BKLF	Nucleic acid binding// zinc ion binding
-1.86	0.0003	Foxp1	Forkhead box P1	Nucleic acid binding// transcription factor activity// zinc ion binding
-1.98	0.0341	Luc7l2	LUC7-like 2 (*S. cereviciaie*)	Protein binding// zinc ion binding
-2.41	0.0403	LOC100045546	Similar to Id4	//
-3	0.0336	Cyp1b1	Cytochrome P450, family 1 subfamily b, polypeptide 1	Monooxigenase activity// iron ion binding// electron carrier activity

Table 4.4 Bioconductor analysis of RNA expression profile of murine ES cells at 4h infection compared to 2h

Gene list resulting from the Bioconductor analysis comparing the expression profiles of murine ES cells at 2h and 4h infection. This analysis identified 39 differentially expressed genes, of which 33 have been annotated and therefore reported here. (* = gene reported twice; ** = gene reported three times)

Fold Change	Adj. p value	Gene Symbol	Gene Name	Process and Functions
2.11	0.00	Hspa1b**	heat shock protein 1B	DNA repair /// anti-apoptosis /// response to stress /// response to heat /// negative regulation of caspase activity
1.98	0.02	Ccng2	cyclin G2	cell cycle /// mitosis /// cell division /// regulation of cell cycle
1.97	0.01	LOC638050 /// Zbtb40	zinc finger and BTB domain containing 40 /// similar to zinc finger and BTB domain containing 40	nucleic acid binding /// protein binding /// zinc ion binding /// metal ion binding
1.78	0.00	Herpud1*	homocysteine-inducible, endoplasmic reticulum stress-inducible, ubiquitin-like domain member 1	protein modification process /// response to stress /// response to unfolded protein /// response to unfolded protein
1.75	0.00	Ankrd37	ankyrin repeat domain 37	---
1.69	0.00	Xbp1**	X-box binding protein 1	transcription /// regulation of transcription, DNA-dependent
1.55	0.02	C430002E04 Rik	RIKEN cDNA C430002E04 gene	---
1.50	0.05	Gdap10	ganglioside-induced differentiation-associated-protein 10	---
-1.52	0.04	Klf10	Kruppel-like factor 10	regulation of transcription, DNA-dependent /// positive regulation of osteoclast differentiation /// zinc-metal ion binding
-1.52	0.01	Zbtb7a	zinc finger and BTB domain containing 7a	negative regulation of transcription from RNA polymerase II promoter /// negative regulation of transcription, DNA-dependent /// zinc ion binding
-1.52	0.04	Gm505	Gene model 505, (NCBI)	---
-1.54	0.04	Lrpap1*	low density lipoprotein receptor-related protein associated protein 1	receptor activity /// heparin binding /// low-density lipoprotein receptor binding /// membrane protein
-1.56	0.01	1810013L24 Rik	RIKEN cDNA 1810013L24 gene	---
-1.56	0.00	Nodal	nodal	negative regulation of transcription from RNA polymerase II promoter // positive regulation of cell proliferation // anterior/posterior pattern formation // stem cell maintenance // negative regulation of cell differentiation /// cytokine activity // growth factor activity
-1.58	0.00	Snai1	snail homolog 1 (Drosophila)	multicellular organismal development // nucleic acid binding // zinc ion binding
-1.58	0.04	Sesn2	sestrin 2	cell cycle arrest

-1.59	0.02	Elf3	E74-like factor 3	regulation of transcription, DNA-dependent /// inflammatory response /// embryonic development /// cell differentiation /// epithelial cell differentiation /// transcription factor activity/// protein binding
-1.61	0.02	Pcmtd1	protein-L-isoaspartate (D-aspartate) O-methyltransferase domain containing 1	protein modification process /// methyltransferase activity
-1.68	0.00	Slc7a1	solute carrier family 7 (cationic amino acid transporter, y+ system), member 1	receptor activity /// amino acid transmembrane transporter activity /// arginine transmembrane transporter activity
-1.70	0.00	Foxp1	forkhead box P1	negative regulation of transcription from RNA polymerase II promoter /// pre-B cell differentiation /// positive regulation of immunoglobulin production /// regulation of transcription, DNA-dependent ///embryonic development /// immunoglobulin V(D)J recombination /// positive regulation of epithelial cell proliferation
-1.71	0.03	Rnase4	ribonuclease, RNase A family 4	positive regulation of endothelial cell proliferation /// activation of phospholipase C activity /// multicellular organismal development actin filament polymerization /// activation of phospholipase A2 /// positive regulation of protein secretion/// nucleic acid binding/// receptor binding/// basal lamina
-1.78	0.04	Arl4a	ADP-ribosylation factor-like 4A	small GTPase mediated signal transduction/// GTPase activity
-1.80	0.00	Aff1	AF4/FMR2 family, member 1	transcription /// positive regulation of transcription, DNA-dependent
-1.97	0.02	Ndrg1	N-myc downstream regulated gene 1	mast cell activation
-2.06	0.00	Cdkn1a	cyclin-dependent kinase inhibitor 1A (P21)	G1/S and G2/M transition of mitotic cell cycle /// response to DNA damage stimulus /// cell cycle arrest /// positive regulation of B cell proliferation /// cellular response to extracellular stimulus /// negative regulation of apoptosis /// positive regulation of fibroblast proliferation /// protein kinase inhibitor activity
-2.10	0.00	Zfp296	zinc finger protein 296	nucleic acid binding /// zinc ion binding
-2.35	0.00	Klf3 /// LOC100046855	Kruppel-like factor 3 (basic) /// similar to BKLF	transcription /// regulation of transcription, DNA-dependent
-2.49	0.00	LOC100046855	similar to BKLF	nucleic acid binding /// zinc ion binding
-2.60	0.02	LOC100045546	similar to Id4	---
-13.13	0.00	Cyp1b1*	cytochrome P450, family 1, subfamily b, polypeptide 1	monooxigenase activity/// iron ion binding /// oxidoreductase activity aromatic compound metabolic process /// metal ion binding
-22.66	0.00	Cyp1a1	cytochrome P450, family 1, subfamily a, polypeptide 1	oxidation reduction /// monooxidoreductase activity/// electron carrier activity /// metal ion binding

4.3.4.1.2 InnateDB pathways analysis

InnateDB has been developed to facilitate systems-level investigations of the innate immune response in human and mice. Its goal is to provide a manually-curated database of the genes, proteins and, particularly, the interactions and signaling responses involved in the mammalian innate immune response. InnateDB is freely available to the public as a tool for innate immunity research where users can search for particular genes or proteins of interest and their relative interactions and pathways [InnateBD: http://innatedb.ca/index.jsp] (Lynn *et al.*, 2008). For this analysis the corresponding human ortholog genes were used since more than 3 quarters of the interactions reported in InnateDB are for *Homo sapiens*. The list of all probes with their respective p-value and the expression fold change determined by pair-comparison of mouse ES cell mRNA expressed at 4h post-infection with *S.* Typhimurium versus uninfected cells, were up-loaded and analyzed using InnateDB. The gene expression values obtained at 2 hours infection and those obtained comparing 4 hours to 2 hours were also analyzed with InnateDB. The pathways obtained were further 'enriched' using the 'over-representation' analysis which uses the genes' fold expression (+/- 1.5) and p-value (<0.1) in order to evaluate the proportion of differentially expressed genes for each pathway (using the default settings for the analysis algorithm: Hypergeometric and the correction method: Benjamini Hochberg).

Table 4.5 InnateDB analysis of genes expressed by murine ES cells at 2h infection with *S.* Typhimurium

The analysis reported only up-regulated pathways at 2h infection of AB2.2 murine ES cells with *S.* Typhimurium SL1344, although they are not statistically significant (corrected p-value).

Name of Pathway up-regulated at 2h infection of AB2.2	Source Name	Pathway uploaded gene count	Pathway up-regulated genes count	Pathway up-regulated p-value	Pathway up-regulated p-value (corrected)
P450 Epoxidations	REACTOME	3	1	0.000602	0.790329
Metabolism of xenobiotics by cytochrome P450	KEGG	28	1	0.005618	1.000000
Tryptophan metabolism	KEGG	52	1	0.010433	1.000000

Table 4.6 InnateDB pathway analysis of murine ES cells expression profile at 4h infection: up-regulated pathways

The whole gene list derived from Bioconductor analysis of the expression data at 4h infection with *S.* Typhimurium SL1344 versus uninfected AB2.2 murine ES cells (0h) was used for this analysis. The analysis did not reveal significantly up-regulated pathways according to adjusted p-values.

Name of pathway up-regulated at 4h infection of AB2.2	Source Name	Pathway uploaded gene count	Pathway up-regulated genes count	Pathway up-regulated p-value	Pathway up-regulated p-value (corrected)
Lipoic acid metabolism	KEGG	3	1	0.006008	1
Ubiquitin mediated proteolysis	KEGG	127	2	0.025359	1
Circadian rhythm	KEGG	13	1	0.025802	1
Sprouty regulation of tyrosine kinase signals	PID BIOCARTA	17	1	0.033620	1
Er associated degradation (erad) pathway	PID BIOCARTA	18	1	0.035566	1
Pkc-catalyzed phosphorylation of inhibitory phosphoprotein of myosin phosphatase	PID BIOCARTA	20	1	0.039446	1
EGFR downregulation	REACTOME	22	1	0.043313	1
Maturity onset diabetes of the young	KEGG	23	1	0.045241	1
Rho cell motility signaling pathway	PID BIOCARTA	31	1	0.060540	1
Rac1 cell motility signaling pathway	PID BIOCARTA	35	1	0.068106	1
N-Glycan biosynthesis	KEGG	38	1	0.073745	1

Table 4.7 InnateDB pathway analysis of murine ES cells expression profile at 4h infection: down-regulated pathways

The genes resulting from the analysis of gene expression at 4h infection compared to uninfected AB2.2 murine ES cells were analyzed with InnateDB. The pathway analysis did not reveal any statistically significantly for down regulated pathway after p-value adjustment.

Name of Pathway down-regulated at 4h infection of AB2.2	Source Name	GO term uploaded gene count	GO term down-regulated genes count	GO term down-regulated p-value	GO term down-regulated p-value (corrected)
P450 Epoxidations	REACTOME	3	1	0.003007	1
Gene expression of IL2 by AP-1	INOH	5	1	0.005008	1
TGF-beta Receptor Signaling Pathway	NETPATH	130	2	0.006412	1
Pertussis toxin-insensitive ccr5 signaling in macrophage	PID BIOCARTA	7	1	0.007006	1
Tsp-1 induced apoptosis in microvascular endothelial cell	PID BIOCARTA	7	1	0.007006	1
Il 3 signaling pathway	PID BIOCARTA	8	1	0.008003	1
JNK cascade	INOH	10	1	0.009996	1

Table 4.8 InnateDB analysis of genes expressed by murine ES cells at 4h infection with *S.* Typhimurium compared to 2h: up-regulated pathways

The analysis reported one up-regulated pathway at 4h versus 2h infection of AB2.2 murine ES cells with *S.* Typhimurium SL1344, although the corrected p-value is not statistically significant.

Name od Pathway up-regulated at 4h vs.2h	Source Name	Pathway uploaded gene count	Pathway up-regulated genes count	Pathway up-regulated p-value	Pathway up-regulated p-value (corrected)
Lipoic acid metabolism	KEGG	3	1	0.000602	0.790329

Table 4.9 InnateDB analysis of genes expressed by murine ES cells at 4h infection with *S.* Typhimurium compared to 2h: down-regulated pathways

The analysis reported a few down-regulated pathways at 4h versus 2h infection of AB2.2 murine ES cells with *S.* Typhimurium SL1344, although the corrected p-value is not statistically significant.

Name of Pathway down-regulated at 4h vs. 2h	Source Name	Pathway uploaded gene count	Pathway up-regulated genes count	Pathway down-regulated p-value	Pathway down-regulated p-value (corrected)
P450 Epoxidations	REACTOME	3	1	0.002406	1
Downregulated of mta-3 in er-negative breast tumors	PID BIOCARTA	15	1	0.011988	1
Metabolism of xenobiotics by cytochrome P450	KEGG	28	1	0.022290	1
Tryptophan metabolism	KEGG	52	1	0.041097	1
Viral Messenger RNA Synthesis	REACTOME	59	1	0.046531	1
Adherens junction	KEGG	70	1	0.055023	1
TGF-beta signaling pathway	KEGG	76	1	0.059632	1

4.3.4.1.3 Real time RT-RCR to confirm Bioconductor analysis

Real time Reverse Transcription (RT) followed by polymerase chain reaction (PCR) is a powerful tool for the detection and quantification of mRNA. It is important to confirm bioinformatics analysis with an alternative method although this has been the centre of debate in the scientific community (Allison *et al.*, 2006; Rajeevan *et al.*, 2001). The total RNA extracted from the *S.* Typhimurium infected cells and uninfected controls was subjected to RT-PCR analysis in order to confirm the data obtained from the microarray study and subsequent Bioconductor analysis. The total RNA was reverse transcribed using QuantiTect (QIAGEN). A SYBR Green-based detection reaction was used and the data were analysed using the ΔΔCt value method developed by Perkin Elmer (Applied Biosystems) to measure the relative quantification of a target gene in comparison to a reference gene. This method is an approximation of the RNA quantity assuming that RT-PCR reaction efficiencies are all equal to 2 (i.e. that each cycle of PCR results in two-fold increase in the number of RNA species). The fold change of the target genes were then calculated in relation to the expression of the internal control gene chosen, β-actin in this study, using the equation "ratio=$2^{-\Delta\Delta Ct}$" where Ct is the thermo cycle at which the green fluorescence dye is first detectable and 2 represents the reaction efficiency. A few genes determined to be significantly up- or down-regulated by microarray nalysis were chosen to be confirmed by semi-quantitative RT-PCR. The genes were selected in order to cover a representive set of genes or pathways exhibiting differential expression. These genes were involved in cholesterol metabolism, cell-cycle regulation, stress responses, apoptosis regulation and transcription factors. For a more detailed description of each gene please refer to Table 4.3.

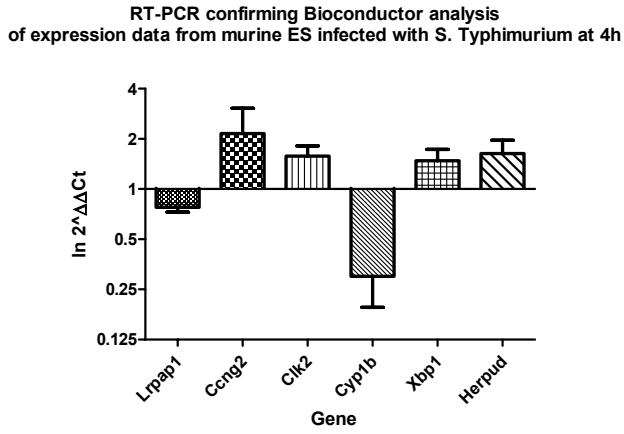

Figure 4.5 RT-PCR results conducted on representative genes identified by the Bioconductor analysis of genes differentially expressed at 4h infection vs. uninfected cells

A few genes with high fold change and significantly differentially expressed during infection, revealed through Bioconductor analysis, were chosen for relative quantification using RT-PCR. In this analysis the Ct values of the target genes were compared to the Ct value of an internal control gene, β-actin, and the ratios calculated and plotted as $ln2^{\wedge -\Delta\Delta ct}$. The reactions were carried out in triplicate for each biological replicate at 0h and 4h infection and are reported here as the mean values. The error bars represent the standard error for each replicate. The initial amount of template cDNA is inversely proportional to the parameter measured for each reaction, which is the threshold cycle (Ct).

4.3.4.1.4 Statistical analysis of RT-PCR data on genes identified by Bioconductor

Statistical analysis of the RT-PCR results was carried out using the online Relative expression software tool (REST©), and the results can be found in Figure 4.6. This mathematical model compares two groups with up to 16 data points in a sample and 16 in a control group, and is based on the PCR efficiencies and the mean Ct deviation between the sample and the control group (Herrmann & Pfaffl, 2005). Subsequently, the expression ratio results of the investigated transcripts are tested for significance using a randomization test. Permutation or randomization tests are a useful alternative to more standard parametric tests for analysing experimental data. They have the advantage of making no distributional assumptions about the data, while remaining as powerful as parametric tests (Pfaffl *et al.*, 2002).

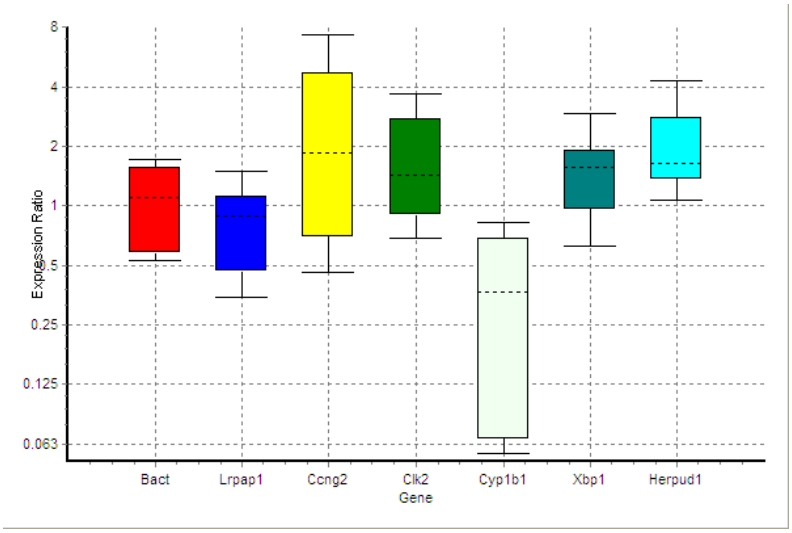

Figure 4.6 Whisker box plot of the RT-PCR results for the Bioconductor-generated differentially expressed genes

The Ct values obtained from RT-PCR for a few of the genes that were identified Bioconductor analysis as differentially expressed in AB2.2 mouse ES cells at 4h invasion with *S.* Typhimurium were statistically investigated by REST©. The random statistical analysis was performed using the triplicate mean values from three different biological replicates; however none of the genes' expression was significantly different in comparison to the internal control gene β-actin.

RT-PCR meant to confirm the results obtained by bioinformatics analysis of up- or down-regulated genes. In this case the genes chosen to be confirmed showed the higher difference in fold expression at 4h infection. However, statistical analysis didn't highlight a significant difference between the level of expression of the genes at 0h and at 4h.

4.3.4.2 GeneSpring analysis

4.3.4.2.1 Results from GeneSpring pair-comparison analysis

In our laboratory microarray data were historically analyzed by GeneSpring. The Agilent GeneSpring version 7.3.1 platform is an expression analysis tool. Here it was used to analyse the Affymetrix Mouse GeneChip® 430 2.0 Array used to investigate the murine AB2.2 ES cell RNA expression profile during *S.* Typhimurium infection at 2h and 4h post-infection.

The array QC is shown in Appendix A. The data were first normalized using GCRMA (Wu *et al.*, 2004), which takes into consideration GC content, and then the data was then filtered using the Benjamini-Hochberg false discovery rate (FDH) method, which assumes independent p-values across genes; the genes were filtered for confidence p-value < 0.05. This procedure provides a good balance between discovery of significant genes and protection against false positives, since the occurrence of the latter is confined to a small proportion of the list, and it is the best choice of multiple-testing correction for most analyses (GeneSpring Manual).

Table 4.10 GeneSpring analysis of the mRNA expression profile of AB2.2 murine ES cells at 2h infection

This comparative analysis revealed 26 genes significantly differentially regulated for p-value < 0.05 and fold expression change of +/- 1.5. 19 annotated genes are reported here. (* = reported twice; ** = reported three times)

Genes selected from condition Time 2.0 that have Normalised Data values that are greater or less than those in condition(s) Time 0.0 by a factor of 1.5 fold. Starting gene list: Filter for confidence t-test p-value 0 - 0.05, Benj and Hoch FDR, 1 cond of 3.

Fold Change	Common	Description	Biological Process and or Molecular Function
8.91	Cyp1a1	cytochrome P450, family 1, subfamily a, polypeptide 1	electron transport// monooxygenase activity; oxidoreductase activity// ER
3.52	Cyp1b1*	cytochrome P450, family 1, subfamily b, polypeptide 1	oxidation reduction /// electron carrier /// ER
1.97	Nfkbiz	nuclear factor of kappa light polupeptide gene enhancer in B-cells inhibitor, zeta	inflammatory response // regulation of transcription // DNA binding
1.66	Clstn3	calsyntenin 3	cell adhesion // ER // Golgi apparatus // calcium ion binding // protein binding
1.65	Anpep	alanyl (membrane) aminopeptidase	proteolisis and peptidolysis // zinc ion binding
1.65	Map3k3	mitogen-activated protein kinase kinase kinase 3	protein amino acid autophosphorylation // ATP binding // kinase activity
1.64	Mark2	MAP/microtubule affinity-regulating kinase 2	cell differentiation // ATP binding // kinase activity
1.59	Slc6a6	solute carrier family 6 (neurotransmitter transporter, taurine), member 6	beta-alanine transport // integral to plasma membrane
1.59	Lpp	LIM domain containing preferred translocation partner in lipoma	cell adhesion // cell junction // metal ion binding // protein binding
1.56	Klf3*	Kruppel-like factor 3 (basic)	regulation of transcription // zinc ion binding
1.55	Zfp296	zinc finger protein 296	//
1.55	Snai1	snail homolog 1 (Drosophila)	development // DNA binding // zinc ion binding
1.54	Inf2	inverted formin, FH2 and WH2 domain containing	actin cytoskeleton organization and biogenesis // actin binding // Rho GTPase binding
1.53	Pdpk1	3-phosphoinositide dependent protein kinase-1	ATP binding // protein serine/threonine kinase activity // signal transduction // cytoplasmic vescicle //
1.52	Synj1	Synaptojanin 1	endocytosis // clathrin coat // cytoplasm // hydrolase activity // inositol or phosphatidylnositol phosphatase activity
1.51	Mint	Msx2 interacting nuclear target protein	regulation of transcription from Pol II promoter // binds G/T-rich dsDNA and ssDNA // mitochondrial inner membrane // nucleus
-1.59	Xist	inactive X specific transcripts	dosage compensation by inactivation of X chromosome
-1.62	Tpd52l2	tumor protein D52-like 2	//

Table 4.11 GeneSpring analysis of the mRNA expression profile of AB2.2 murine ES cells at 4h infection

A total of 89 genes were revealed to be differentially expressed by murine AB2.2 ES cells at 4h infection with *S.* Typhimurium SL1344. 56 annotated genes are reported here. The genes were filtered for p-value < 0.05 and fold change +/- 1.5. A few genes are repeated, as indicated by asterisks, and this is a sign that a gene is particularly relevant (* = reported twice; ** = reported three times).

Genes selected from condition Time 4.0 that have Normalised Data values that are greater or less than those in condition(s) Time 0.0 by a factor of 1.5 fold. Starting gene list: Filter for confidence t-test p-value 0 - 0.05, Benj and Hoch FDR, 1 cond of 3.

Fold Change	Common	Description	Biological Process and or Molecular Function
2.43	Banp	Btg3 associated nuclear protein	protein binding
2.17	Hspa1b**	heat shock protein 1A	anti-apoptosis; inhibition of caspase activation; ATP binging
2.03	Ccng2*	cyclin G2	cell cycle regulation
1.83	Pdxp	pyridoxal (pyridoxine, vitamin B6) phosphatase	catalytic activity // metabolic process
1.82	Stat2	signal transducer and activator of transcription 2	involved in signal transduction and transcription for type I interferon signaling
1.73	AA408868	expreexpressed sequence AA408868	inflammatory response; regulation of transcription, DNA-dependent
1.71	Ier3	immediate early response 3	integral membrane
1.69	Herpud1*	homocysteine-inducible, endoplasmic reticulum stress-inducible, ubiquitin-like domain member 1	response to stress // response to unfolded protein // ER membrane
1.66	Mrpl29/ 1200010C09Rik	mitochondrial ribosomal protein L49	translation /// structural component of ribosome
1.59	Cnnm3*	cyclin M3	ion transport // integral to membrane
1.57	Sel1h	Sel1 (suppressor of lin-12) 1 homolog (C. elegans)	Notch signaling pathway // endoplasmic reticulum // extracellular space
1.56	Socs3	suppressor of cytokine signaling 3	intracellular signaling cascade; regulation of cell growth; signal transduction
1.56	Meg3	maternally expressed 3	
1.54	Lyst	lysosomal trafficking regulator	cellular defense response // response to bacterium // cytoplasm
1.54	1200010C09Rik	RIKEN cDNA 1200010C09 gene	response to unfolded protein// ubiquitin-protein ligase activity
1.54	BC018601	cDNA sequence BC018601	
1.54	Aof1	amine oxidase, flavin containing 1	oxidation reduction // electron carrier // metal ion binding
1.53	Xbp1	X-box binding protein 1	regulation of transcription DNA-dependent
1.52	Eif2ak3	eukaryotic translation initiation factor 2 alpha kinase 3	eIF2a kinase // electron transport// kinase activity // ATP binding
1.52	Cebpd	CCAAT/enhancer binding protein (C/EBP), delta	transcription regulation // DNA binding
1.52	Tbl2	transducin (beta)-like 2	extracellular space
1.52	Zc3h10	zinc finger CCCH type containing 10	metal ion binding // nucleic acid binding
1.51	Mkx	mohawk homeobox	multicellular organismal development // DNA binding
1.51	Irf2bp1	interferon regulatory factor 2 binding protein 1	negative regulation of transcription from Pol II promoter
1.5	Clk2	CDC-like kinase 2	autophosphorylation; protein amino acid phosphorylation// ATP binding; kinase activity
1.5	Hspa1a	heat shock protein 1A	DNA repair // response to heat // ATP binding

-1.5	Spic	Spi-C transcription factor (Spi-1/PU.1 related)	DNA binding; transcription factor activity
-1.5	Sfrs5	splicing factor, arginine/serine-rich 5 (SRp40, HRS)	spicesome // mRNA splice site selection // nucleic acid binding
-1.51	Cphx	cytoplasmic polyadenylated homeobox	transcription regulation // DNA binding
-1.52	Chic2	platelet derived growth factor receptor, alpha polypeptide	Golgi to plasma membrane transport // Golgi-associated vescicle
-1.52	Plaur	urokinase plasminogen activator receptor	binding of urokinase// cell surface receptor// kinase activity
-1.52	Plxdc1	plexin domain containing 1	receptor activity // integral to membrane
-1.54	Foxd3	forkhead box D3	DNA binding // transcription factor activity
-1.54	Mllt6	myeloid/lymphoid or mixed lineage-leukemia translocation to 6 homolog (Drosophila)	transcription regulation // DNA binding // metal ion binding
-1.54	Txnip	thioredoxin interacting protein	response to oxidative stress// anzyme inhibitor activity
-1.56	Cirbp	cold inducible RNA binding protein	RNA binding // nucleic acid binding
-1.56	Lrpap1*	low density lipoprotein receptor-related protein associated protein 1	heparin binding // low-density lipoprotein receptor binding // cytoplasm // ER// contain alpha-2-macroglobulin RAP domain
-1.57	Idb2	inhibitor of DNA binding 2	protein binding // transcription regulation
-1.58	Luc7l2	LUC7-like 2 (S. cerevisiae)	
-1.58	Rpl27a	ribosomal protein L27a	translcation // cytosolic ribosome
-1.59	Arl4a	ADP-ribosylation factor-like 4	small-GTPase mediate signal transduction // GTP binding
-1.64	Rnpc2	RNA-binding region (RNP1, RRM) containing 2	mRNA processing // nuclear mRNA splicing via spliceosome // regulation of transcription
-1.64	Idb3	inhibitor of DNA binding 3	negative regulation of transcription from Pol II promoter
-1.67	Ndrg1*	N-myc downstream regulated 1	mast cell activation // cytoplasm-nucleus
-1.7	Wac	WW domain containing adaptor with coiled-coil	sliceosome // protein binding
-1.76	Foxp1	forkhead box P1	cell differentiation // DNA binding // metal ion binding
-1.76	Klf3	Kruppel-like factor 3 (basic)	transcription regulation // DNA binding // metal ion binding
-1.81	Nab2	Ngfi-A binding protein 2	negative regulation of transcription // regulation of transcription DNA-dependent
-1.82	Slc30a1	solute carrier family 30 (zinc transporter), member 1	cation transport; zinc ion transport
-1.9	Tiparp	TCDD-inducible poly(ADP-ribose) polymerase	NAD + ADP ribosiltransferase activity // metal ion binding // nucleus
-1.94	Luc7l2	LUC7-like 2 (S. cerevisiae)	metal ion binding // protein binding
-2	Cyp1a1	cytochrome P450, family 1, subfamily a, polypeptide 1	electron transport// monooxygenase activity; oxidoreductase activity// ER
-2.18	Idb4**	inhibitor of DNA binding 4	cell proliferation // protein binding // transcription regulation
-2.29	Slc30a1	solute carrier family 30 (zinc transporter), member 1	cation transport // cellular zinc ion homeostasis // integral to membrane
-2.32	Pou4f2	POU domain, class 4, transcription factor 2	axon extension involved in development // chromatin binding
-2.82	Cyp1b1*	cytochrome P450, family 1, subfamily b, polypeptide 1	oxidation reduction // electron carrier // ER

Table 4.12 GeneSpring analysis of the mRNA expression profile of AB2.2 murine ES cells at 4h vs. 2h infection

GeneSpring analysis results of murine ES cell genes differentially expressed at 4h infection vs. 2h infection with S. Typhimurium. The genes were filtered for p-value < 0.05 and fold change +/- 1.5. Genes reported more than once are indicated by asterisks (* = reported twice; ** = reported three times).

Genes selected from condition Time 4.0 that have Normalised Data values that are greater or less than those in condition(s) Time 2.0 by a factor of 1.5 fold. Starting gene list: Filter for confidence t-test p-value 0 - 0.05, Benj and Hoch FDR, 1 cond of 3. In total 87 genes were differentially expressed of which 63 were previously annotated

Fold Change	Common	Description	Biological Process and or Molecular Function
2.02	Hspa1b**	heat shock protein 1A	anti-apoptosis // inhibition of caspase activation // response to heat // ATP binding // chaperon activity
1.85	Banp	Btg3 associated nuclear protein	protein binding
1.78	Ccng2	cyclin G2	cell cycle regulation // cyclin-dependent protein kinase regulator activity
1.72	Ier3	immediate early response 3	integral to membrane
1.7	Zbtb40	zinc finger and BTB domain containing 40	nucleus// metal ion binding // zinc ion binding
1.69	Cebpd	CCAAT/enhancer binding protein (C/EBP), delta	regulation of transcription// DNA binding // protein dimerization activity // nucleus
1.68	Gadd45g	growth arrest and DNA-damage-inducible 45 gamma	T-helper 1 cell differentiation // activation of MAPKK // apoptosis // interferon-gamma biosynthesis // negative regulation of protein kinase activity // protein biosynthesis // regulation of cell cycle // nucleus // structural constituent of ribosome
1.65	Ankrd37	ankirin repeat domain 37	cytoplasm // nucleus
1.64	Herpud1*	homocysteine-inducible, endoplasmic reticulum stress-inducible, ubiquitin-like domain member 1	protein modification // response to stress // ER membrane
1.64	Mkx	mohawk homeobox	multicellular organismal development // DNA binding
1.64	Xbp1**	X-box binding protein 1	regulation of transcription DNA-dependent
1.59	Tnfsf11	tumor necrosis factor (ligand) superfamily, member 11	regulates osteoclast differentiation and activation // immune response // cytokine activity // protein binding // tumor necrosis factor receptor binding // integral to membrane
1.58	Pdxp	pyridoxal (pyridoxine, vitamin B6) phosphatase	catalytic activity // metabolic process
1.52	Purg	purine-rich element binding protein G	nucleus // DNA binding
1.52	L3mbtl3	l(3)mbt-like 3 (Drosophila)	regulation of transcription // nucleus
1.5	Ccng2	cyclin G2	cell cycle regulation
-1.5	Lamp2	lysosomal membrane glycoprotein 2	tRNA aminoacylation for protein translation // integral to membrane; lysosome // ATP binding; tRNA ligase activity
-1.5	Syt11	synaptotagmin 11	transport // cell junction //cytoplasmic vescicle // calcium ion binding
-1.5	Sesn2	sestrin 2	cell cycle arrest // nucleus
-1.51	Spic	Spi-C transcription factor (Spi-1/PU.1 related)	regulation of transcription// transcription factor complex // DNA binding // nucleus
-1.51	Tieg1	TGFB inducible early growth response 1	transcription factor
-1.52	Hist1h1c	histone 1, H1c	chromosome organization and biogenesis // nucleosome // DNA binding // protein binding
-1.52	Frmd4a	FERM domain containing 4A	cytopasm // cytoskeleton // binding
-1.52	Idb4	inhibitor of DNA binding 4	cell proliferation // protein binding // transcription regulation
-1.52	Gpr160	G protein-coupled receptor 160	G-protein coupled receptor protein signaling pathway // signaling transduction // integral to

			membrane // receptor activity
-1.53	Luc7l2	LUC7-like 2 (S. cerevisiae)	metal ion binding // protein binding
-1.53	Bcor	Bcl6 interacting corepressor	chromatin modification // regulation of transcription // DNA binding
-1.55	Daf1	decay accelerating factor 1	complement activation, classical pathway // integral to membrane
-1.56	Flnb	filamin beta	skeletal muscle development // cytoplasm// cytoskeleton // actin binding // protein binding
-1.56	Pwwp2b	PWWP domain containing 2B	//
-1.57	Slc7a1	solute carrier family 7 (cationic amino acid transporter, y + system), number 1	amino acid transport// arginine transport // integral to membrane
-1.57	Trak1	trafficking protein, kinesin binding 1	GABA receptor binding
-1.57	Mapk4	mitogen-activated protein kinase 4	cell cycle // protein amino acid phosphorylation // ATP binding // kinase activity
-1.57	Nodal*	nodal	cytokine activity // growth factor activity // determination of left/right symmetry // development
-1.58	Zbtb7*	zinc finger and BTB domain containing 7	cartilage development // negative regulation of transcription from RNA polymerase II promoter // DNA binding // histone acetyltransferase binding
-1.59	Idb1	inhibitor of DNA binding 1	development // negative regulation of transcription from Pol II promoter // regulation of angiogenesis // nucleus
-1.6	Zmat4	zinc finger, matrin type 4	intracellular // nucleus // DNA binding// metal ion binding
-1.61	Spry4	sprouty homolog 4 (Drosophila)	multicellular organismal development // negative regulation of MAP kinase activity // cytoplasm // membrane // protein binding
-1.63	Foxp1	forkhead box P1	cell differentiation // DNA binding // metal ion binding
-1.63	Socs2	suppressor of cytokine signaling 2	intracellular signaling cascade // negative regulation of multicellular organism growth // growth hormone receptor binding // protein binding
-1.67	Rnase4	ribonuclease, Rnase A family 4	endonuclease activity; hydrolase activity; nucleic acid binding; pancreatic ribonuclease activity
-1.68	Plxdc1	plexin domain containing 1	receptor activity // integral to membrane
-1.69	Nab2	Ngfi-A binding protein 2	transcriptional repressor activity //
-1.69	Cyp2s1	cytochrome P450, family 2, subfamily s, polypeptide 1	monooxygenase activity; oxidoreductase activity // integral to membrane
-1.72	Arl4	ADP-ribosylation factor-like 4	small GTPase mediated signal transduction // intracellular // GTP binding // GTPase activity
-1.73	Mllt2h	homolog of human MLLT2 unidentified gene	transcription factor activity // cell growth and/or maintenance
-1.74	Snai1	snail homolog 1 (Drosophila)	DNA binding; nucleic acid binding; zinc ion binding
-1.76	Mllt6	myeloid/lymphoid or mixed lineage-leukemia translocation to 6 homolog (Drosophila)	regulation of transcription // metal ion binding // DNA binding
-1.8	Pqlc1	PQ loop repeat containing 1	integral to membrane
-1.8	Nr4a1	nuclear receptor subfamily 4, group A, member 1	inhibition of caspase activation // regulation of transcription // steroid hormone receptor activity // nucleus
-1.81	Ccno	cyclin O	DNA repair // hydrolase activity // nucleus
-1.89	Slc30a1	solute carrier family 30 (zinc transporter), member 1	cation transporter activity; zinc ion transporter activity // integral to membrane
-1.95	Ndrg1***	N-myc downstream regulated 1	mast cell activation // cytoplasm // nucleus
-1.96	Cdkn1a	cyclin-dependent kinase inhibitor 1A (P21)	cell cycle arrest // negative regulation of apoptosis // positive regulation of B-cell proliferation // positive regulation of non-apoptotic programmed cell death // response to DNA damage stimulus
-2.06	Zfp296	zinc finger protein 296	//
-2.33	Idb4*	inhibitor of DNA binding 4	//
-2.38	Pou4f2	POU domain, class 4, transcription factor 2	axon extension involved in development // chromatin binding

-2.44	Slc30a1	solute carrier family 30 (zinc transporter), member 1	cation transporter activity // zinc ion transporter activity // integral to membrane
-2.48	Klf3***	Kruppel-like factor 3 (basic)	transcription regulation // DNA binding // metal ion binding
-9.9	Cyp1b1*	cytochrome P450, family 1, subfamily b, polypeptide 1	oxidation reduction // electron carrier // ER
-17.79	Cyp1a1	cytochrome P450, family 1, subfamily a, polypeptide 1	electron transport// monooxygenase activity; oxidoreductase activity // ER

4.3.4.2.2

4.3.4.2.3 Gene Ontology analysis of the genes differentially expressed at 4h

The Gene Ontology (GO) Consortium [http://geneontology.org], maintains a database of controlled vocabularies for the description of molecular functions, biological processes and cellular components of gene products. A gene product can have one or more molecular functions, be used in one or more biological processes, and may be associated with one or more cellular components. The results from GO analysis can provide insights into the biology of the systems being studied.

GO analysis for molecular functions is performed on the genes significantly differentially expressed at 4h infection as determined by GeneSpring analysis. The genes are filtered for p-value < 0.05 and expression fold change greater than +/- 1.5. The GO results appear as a spreadsheet in Table 4.15 that reports the number and the percentage of genes annotated in each category, the number of analyzed genes and a p-value also known as 'enrichment score' per category. The p-value reported indicates the relative importance or significance of the GO term among the entities in the selection compared to the entities in the whole dataset (Ashburner *et al.*, 2000).

The lists of GO analysis for biological processes and cellular components are available in Appendix A.

Table 4.13 Gene Ontology results in the molecular-function category for GeneSpring analysis

The 58 annotated genes, out of 89 total, differentially expressed following 4h of *S.* Typhimurium infection (p-value < 0.05, fold change +/- 1.5) are analyzed.

Filter on 1.5 fold change 4-0h (89 genes, 58 annotated) selected with GO:3674:molecular_function					
GO Category	Genes in Category	% of Genes in Category	Genes in List in Category	% of Genes in List in Category	p-Value
GO:4497: monooxygenase activity	152	0.666	3	5.172	0.00683
GO:16712: oxidoreductase activity	18	0.0789	1	1.724	0.0448
GO:30377: U-plasminogen activator receptor activity	1	0.00438	1	1.724	0.00254
GO:15082: di-, tri-valent inorganic cation transporter activity	44	0.193	2	3.448	0.0056
GO:5385: zinc ion transporter activity	10	0.0438	2	3.448	0.000282
GO:46873: metal ion transporter activity	77	0.337	2	3.448	0.0164
GO:46915: transition metal ion transporter activity	39	0.171	2	3.448	0.00443
GO:1871: pattern binding	125	0.548	2	3.448	0.0403
GO:30247: polysaccharide binding	121	0.53	2	3.448	0.038
GO:5539: glycosaminoglycan binding	119	0.521	2	3.448	0.0369
GO:8201: heparin binding	86	0.377	2	3.448	0.0202
GO:3676: nucleic acid binding	4624	20.26	18	31.03	0.0346
GO:3743: translation initiation factor activity	135	0.591	2	3.448	0.0463
GO:19207: kinase regulator activity	82	0.359	2	3.448	0.0185
GO:19887: protein kinase regulator activity	80	0.35	2	3.448	0.0177
GO:16538: cyclin-dependent protein kinase regulator activity	24	0.105	2	3.448	0.00169
GO:30528: transcription regulator activity	1800	7.885	10	17.24	0.0145
GO:16564: transcriptional repressor activity	164	0.718	3	5.172	0.00841

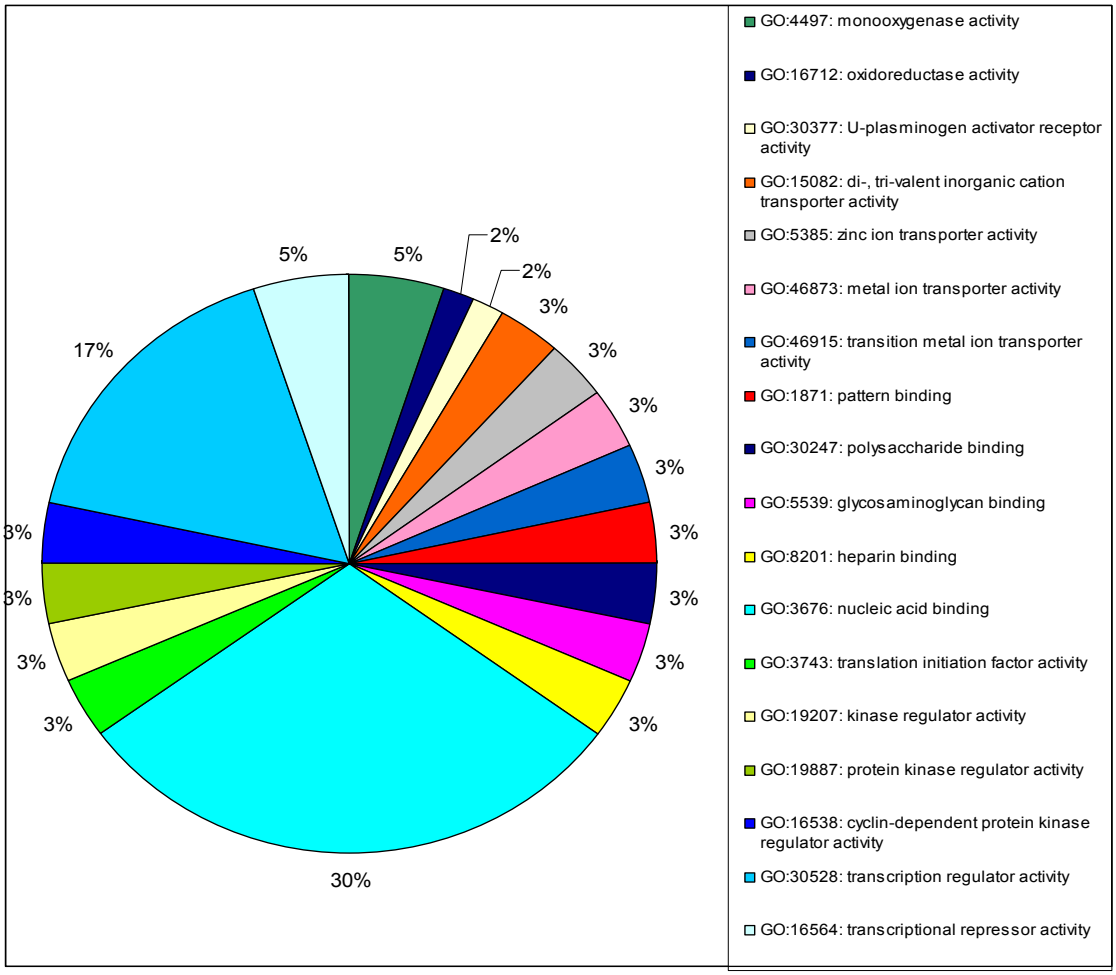

Figure 4.7 Graphical representation of the Gene Ontology analysis for molecular function of genes differentially expressed at 4h

The 89 genes determined to be significantly differentially expressed by GeneSpring analysis of murine AB2.2 ES cells at 4h infection with *S.* Typhimurium, (compared to uninfected controls) were further examined for Gene Ontology annotation describing the molecular function. This analysis highlighted that about a third of the listed genes have 'nucleic acid binding' ability and about a quarter have 'transcription regulator activity'.

4.3.4.2.4 Real time RT-PCR to confirm GeneSpring analysis

The conditions used are the same as previously described for RT-PCR. Briefly, cDNAs were amplified using the QuantiTect QIAGEN kit and the real time RT-PCRs were carried out using the Quantum SYBR Green kit on a Stratagene real time machine. . It is important to validate the results of the bioinformatic analysis and a few genes reported to be significantly up- or down-regulated were selected to be confirmed using the relative quantification method, ΔΔCt. Gene selection was based on their potential relevance to *Salmonella*-host interaction studies suggested by close reading of the literature. These genes were distinct from those identified by Bioconductor analysis. Genes involved in early response, cellular traffiking regulation, cytokine signaling and anti-inflammatory response were included. For a more detailed description of each gene please refer to Table 4.11. The resulting fold changes are reported in Figure 4.8.

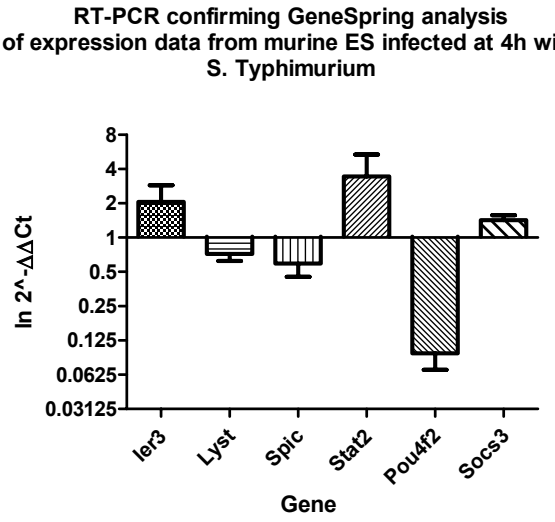

Figure 4.8 RT-PCR results conducted on a few genes identified by GeneSpring analysis

Some of the genes determined by GeneSpring analysis to be up- or down- regulated and with a significant p-value during infection were tested for relative quantification by RT-PCR. In this analysis the Ct values of target genes were compared to the Ct value of an internal control β-actin and the ratios were calculated and plotted as ln $2^{\wedge-\Delta\Delta Ct}$. The reactions were carried out in triplicate for each biological replicate at 0h and at 4h infection and reported here are the mean values. The error bars represent the standard error for each replicate. The initial amount of template cDNA is inversely proportional to the parameter measured for each reaction, the Ct.

Semi-quantitative RT-PCR confirms the results obtained by bioinformatics analysis of up- or down-regulated genes. In this case the genes chosen to be confirmed were identified by Gene Spring analysis as differentially expressed at 4h infection. The RT-PCR results confirmed that those genes reported to be up- or down-regulated by bioinformatics analysis were really up- or down-regulated.

4.3.4.2.5 Statistical analysis of RT-PCR data on genes identified by GeneSpring

Statistical analysis was conducted on the Ct values obtained from the real time RT-PCR conducted on a few genes identified by GeneSpring analysis. The REST© statistical program was used as described before. This analysis indicated that the Ct values of target genes were not significantly (p-value < 0.05) different to the Ct value of the target gene βactin (Figure 4.9). Nevertheless one gene, Pou4f2 reported a p-value < 0.1. This gene contributes to the mantainance of the stemness characteristic. This result suggest that ES cells may be initiating a differentiation process during infection or that bacterial infection induce cell differentiation. However, further supporting evidence would be required to confirm this possibility.

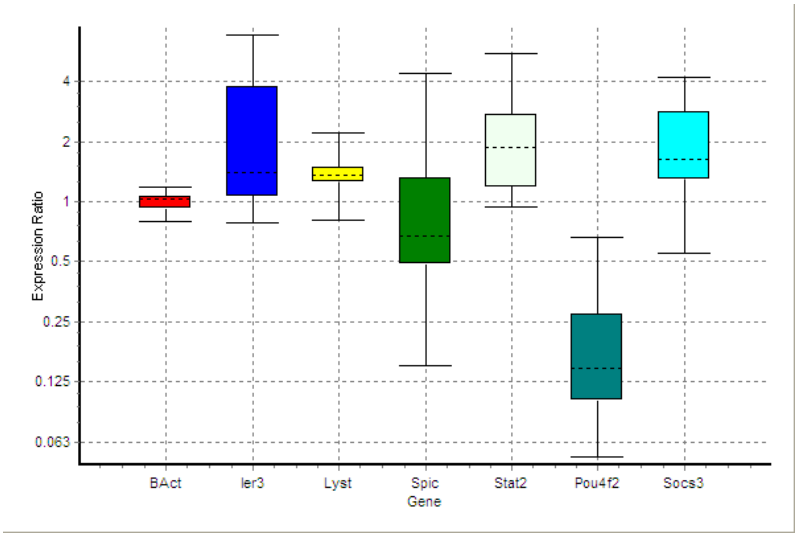

Figure 4.9 Whisker box plot of RT-PCR reaction conducted on genes identified by GeneSpring

This figure represents the Ct mean of three replicate reactions conducted on each gene. The genes were identified by GeneSpring analysis and the expression level of each one was compared to the expression level of an internal control gene: β-actin. In this experiment total RNA extracted from AB2.2 mouse ES cells uninfected and infected at 4h with *S.* Typhimurium SL1344 were used.

4.3.4.3 GEPAS: ASCA analysis

4.3.4.3.1 Time course analysis using ASCA

The mRNA profile of murine ES cells infected with *S.* Typhimurium SL1344 was further examined in a time course analysis. The analysis using time as a variable was carried out in order to highlight interesting expression patterns in gene expression during infection. A similar expression pattern might indicate co-regulation by a common transcription factor. For this purpose the Gene Expression Profile Analysis Suite (GEPAS) [http://www.gepas.org], which has been designed to provide an intuitive web-based interface (Montaner *et al.*, 2006), was employed. The ANOVA-simultaneous component analysis (ASCA) was proposed in order to analyze metabolomics data, and in this study was used in order to take into consideration the 'time' as a variable over the experiment (Smilde *et al.*, 2005). Basically ASCA fits an ANOVA model for each gene. In this case the ANOVA model has two factors, one is the time, which will give the temporal gene expression change related upon treatment, and the other is the individual. This method looks for different expression profile models that a gene can follow during treatment, and can detect if a gene follows the trend very well, but does not necessarily reach a sufficient significance in the traditional way. For a gene to be selected by ASCA, it must follow the trend of the majority of the changing genes (of the 2-3 major patterns). (Dr. Conesa personal communication)

ASCA analysis reported 943 genes, which were grouped into nine arbitrary clusters according to how their expression changed over time during the infection. The trend in each group is reported in Figure 4.10. Each graph reports the expression of the genes contained in each group represented as the mean log2 for each gene's expression divided by its expression at time zero. The three lines represent the three biological replicates. A value of 1 on the y axis represents two-fold up-regulation and a value of -1 represents two-fold down-regulation.

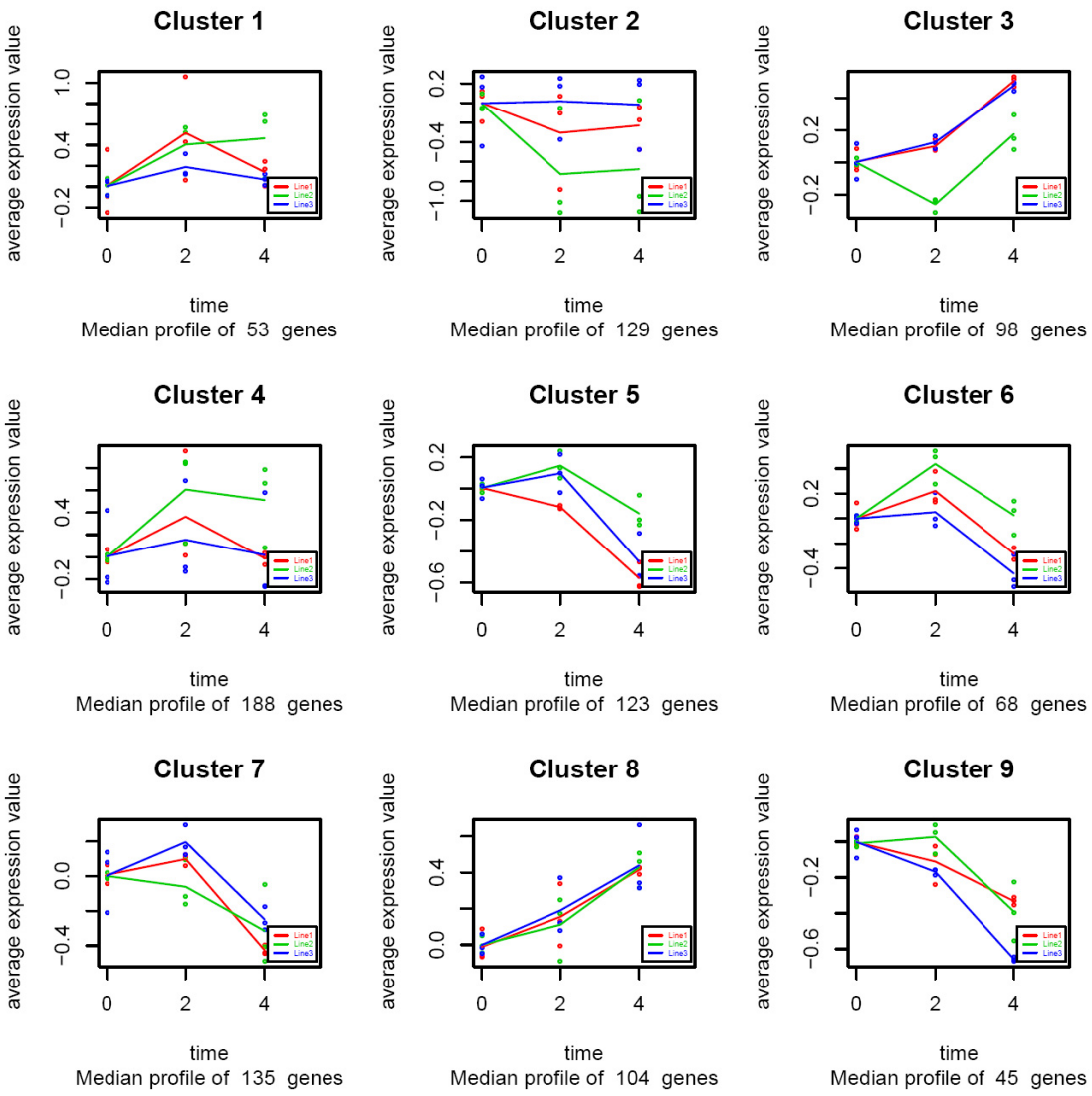

Figure 4.10 Gene clusters derived from ASCA analysis

ASCA analysis was used to investigate the data using time as a variable, and the genes whose expression profile changed during infection are reported. The 953 genes initially listed were then divided into nine arbitrary clusters and only those that best fit each trend were further analyzed.

This study included groups 3 and 8 for up–regulated genes and groups 5, 6, 7 and 9 for down-regulated genes. This analysis revealed 152 genes positively expressed during infection and 271 genes negatively expressed during infection. Tables 4.14 and 4.15 report some of the positively and the negatively regulated genes derived from this analysis, divided in categories that I think are relevant to this study based on current literature. For this reason the genes were organized into six groups: Cyclins, Ubiquitins, Mitochondrion, ER and Golgi apparatus, Cytokines and Chemokines, Cytoskeleton, Immune response and General interest.

Table 4.14 Gene list derived from ASCA analysis of the genes up-regulated during infection

Of the 153 genes found to be up-regulated during infection by ASCA analysis 45 are reported here. The genes are divided in categories that I think are interesting and relevant to this study based on close reading of the literature.

Gene Symbol	Gene Title	Biological and molecular functions
Cyclins		
Ccng2	cyclin G2	regulation of progression through cell cycle /// cell cycle /// mitosis /// cell division/// kinase regularoty activity
Ccnjl	cyclin J-like	regulation of progression through cell cycle
Cnnm3	cyclin M3	biological_process
Ubiquitin		
Herpud1	homocysteine-inducible, endoplasmic reticulum stress-inducible, ubiquitin-like domain member 1	response to stress /// response to unfolded protein /// ER membrane // circadian regulation
Shprh	SNF2 histone linker PHD RING helicase	DNA repair /// nucleosome assembly /// transcription /// ubiquitin cycle /// ATP-binding /// zinc ion binding
Syvn1	synovial apoptosis inhibitor 1, synoviolin	in utero embryonic development /// ubiquitin cycle /// anti-apoptosis /// response to unfolded protein /// multicellular organismal development /// integral to membrane /// ER membrane
Trim32	tripartite motif protein 32	ubiquitin cycle /// nucleic acid binding /// zinc ion binding
Usp26	ubiquitin specific peptidase 26	ubiquitin-dependent protein catabolic process /// ubiquitin cycle
Vps37a	vacuolar protein sorting 37A (yeast)	protein modification process /// ubiquitin cycle /// transport /// protein transport
Armet	arginine-rich, mutated in early stage tumors	ubiquitin cycle /// biological_process
Mitochondrion, ER, Golgi		
Gls	glutaminase	glutamine metabolic process/// mitocondrial inner membrane
Mtus1	mitochondrial tumor suppressor 1	ATP synthesis coupled proton transport /// receptor activity /// proton-transporting two-sector ATPase complex
Bfar	bifunctional apoptosis regulator	anti-apoptosis /// protein binding /// ER
Dhcr7	7-dehydrocholesterol reductase	blood vessel development /// steroid biosynthetic process /// cholesterol biosynthetic process /// lipid biosynthetic process /// regulation of cell proliferation /// nuclear outer membrane and ER
Eif2ak3	eukaryotic translation initiation factor 2 alpha kinase 3	skeletal development /// electron transport /// translation /// protein amino acid phosphorylation /// caspase activation /// virus-infected cell apoptosis /// ER overload response /// response to unfolded protein /// calcium-mediated signaling /// insulin secretion /// protein kinase activity
Ero1lb	ERO1-like beta (S. cerevisiae)	electron transport /// oxidoreductase activity// ER
Gcs1	glucosidase 1	metabolic process /// oligosaccharide metabolic process /// ER /// integral to membrane
Hspa5	heat shock 70kD protein 5 (glucose-regulated protein)	anti-apoptosis /// ER overload response /// negative regulation of caspase activity /// ATP binding /// ribosome binding
Pigc	phosphatidylinositol glycan anchor biosynthesis, class C	GPI anchor biosynthetic process /// transferase activity /// ER membrane
Gopc	golgi associated PDZ and coiled-coil motif containing	transport /// autophagy /// protein transport /// protein homooligomerization /// small GTPase regulator activity /// membrane fraction/// trans-Golgi network transport vescicle
Slc35a5	solute carrier family 35, member A5	carbohydrate transport /// nucleotide-sugar transport /// Golgi membrane
Kif1b	kinesin family member 1B	microtubule-based process /// microtubule-based movement /// nerve-nerve synaptic transmission /// anterograde axon cargo transport /// embryonic development /// cytoskeleton-dependent intracellular transport /// mitochondrion transport along microtubule /// microtubule associated complex/// ATPase activity
Acbd3	acyl-Coenzyme A binding domain containing 3	steroid biosynthetic process /// transport /// acyl-CoA binding /// mitochondrion
EG623661	predicted gene, EG623661	protein modification process /// catalytic activity /// mitochondrion

Cytokine & Chemokine		
Nfat5	nuclear factor of activated T-cells 5	cytokine production /// transcription /// positive regulation of transcription from RNA polymerase II promoter /// protein binding
Tnfsf11	tumor necrosis factor (ligand) superfamily, member 11	immune response /// multicellular organismal development /// lymph node development /// protein homooligomerization /// receptor activity /// cytokine activity /// tumor necrosis factor binding
Cytoskeleton		
Taok2	TAO kinase 2	activation of MAPKK activity /// protein amino acid phosphorylation /// response to stress /// regulation of cell shape /// actin cytoskeleton organization and biogenesis /// positive regulation of JNK cascade /// focal adhesion formation
Actr1b	ARP1 actin-related protein 1 homolog B (yeast)	nucleotide binding /// structural constituent of cytoskeleton /// microtubule associated complex /// actine filament
Elmo2	engulfment and cell motility 2, ced-12 homolog (C. elegans)	phagocytosis /// apoptosis /// cytoskeleton
Enc1	ectodermal-neural cortex 1	proteolysis /// multicellular organismal development /// actin binding /// cysteine-type endopeptidase activity /// cytoskeleton
Hook1	hook homolog 1 (Drosophila)	microtubule cytoskeleton organization and biogenesis /// multicellular organismal development /// actin binding /// microtubule binding /// cytoskeleton
Lyst	lysosomal trafficking regulator	transport /// cellular defense response /// signal transduction /// endosome to lysosome transport /// protein transport /// endosome-microtubule-cytoskeleton
Nisch	nischarin	cell communication /// Rac protein signal transduction /// actin cytoskeleton organization and biogenesis /// negative regulation of cell migration /// receptor activity
Immune-Response and General Interest		
Ier3	immediate early response 3	membrane /// integral to membrane /// integral to membrane
Ier5l	immediate early response 5-like	///
Irf2bp1	interferon regulatory factor 2 binding protein 1	negative regulation of transcription from RNA polymerase II promoter
Ppp1r13b	protein phosphatase 1, regulatory (inhibitor) subunit 13B	induction of apoptosis /// defense response /// negative regulation of progression through cell cycle
Apaf1	apoptotic peptidase activating factor 1	neural tube closure /// proteolisis /// apoptosis /// caspase activation /// defense response /// multicellular organismal development /// regulation of apoptosis
Bcl3	B-cell leukemia/lymphoma 3	protein import into nucleus, translocation /// follicular dendritic cell differentiation /// marginal zone B cell differentiation /// humoral immune response mediated by circulating immunoglobulin /// transcription /// antimicrobial humoral response /// positive regulation of interferon-gamma production /// T-helper 1 type immune response /// negative regulation of tumor necrosis factor biosynthetic process /// defense response to bacterium /// regulation of apoptosis /// T-helper 2 cell differentiation /// positive regulation of interleukin-10 biosynthetic process ///
Banp	Btg3 associated nuclear protein	protein binding
Ercc4	excision repair cross-complementing rodent repair deficiency, complementation group 4	DNA metabolic process /// DNA repair /// nucleotide-excision repair /// endonuclease activity /// endodeoxyribonuclease activity /// hydrolase activity
Gbp6	guanylate binding protein 6	immune response /// nucleotide binding /// GTPase activity
Hsp110	heat shock protein 110	response to heat /// chaperone cofactor-dependent protein folding /// nucleotide binding /// ATP binding
Hspa1a	heat shock protein 1A	telomere maintenance /// DNA repair /// protein folding /// response to heat /// ATP binding
Hspa1b	heat shock protein 1B	telomere maintenance /// DNA repair /// protein folding /// anti-apoptosis /// response to heat /// negative regulation of caspase activity /// ATP binding

Table 4.15 Gene list derived from ASCA analysis of genes down-regulated during infection

ASCA analysis highlighted 270 genes negatively regulated during *S.* Typhimurium infection. Potentially genes are organized into categories.

Gene Symbol	Gene Title	Biological and molecular functions
Cyclins		
Ccnt1	cyclin T1	regulation of progression through cell cycle /// regulation of cyclin-dependent protein kinase activity /// transcription /// protein amino acid phosphorylation /// cell cycle
Ccnu	cyclin U	regulation of progression through cell cycle /// DNA repair /// response to DNA damage stimulus /// metabolic process
Cdkn1a	cyclin-dependent kinase inhibitor 1A (P21)	regulation of progression through cell cycle /// response to DNA damage stimulus /// negative regulation of cell proliferation /// positive regulation of B cell proliferation /// negative regulation of apoptosis /// positive regulation of non-apoptotic programmed cell death
Hmox1	heme oxygenase (decycling) 1	heme oxidation /// response to stimulus /// iron ion binding /// ER /// integral membrane
Ubiquitin		
Cbx4	chromobox homolog 4 (Drosophila Pc class)	chromatin assembly or disassembly /// transcription /// ubiquitin cycle /// chromatin modification
Nfkbia	nuclear factor of kappa light chain gene enhancer in B-cells inhibitor, alpha	protein import into nucleus, translocation /// lipopolysaccharide-mediated signaling pathway /// response to lipopolysaccharide /// regulation of cell proliferation /// response to exogenous dsRNA /// negative regulation of myeloid cell differentiation /// negative regulation of Notch signaling pathway /// NF-kappaB bining
Ranbp2	RAN binding protein 2	protein folding /// ubiquitin cycle /// intracellular transport /// protein binding /// metal ion binding
Rnf103	ring finger protein 103	ubiquitin cycle /// nucleic acid binding /// protein binding /// metal ion binding
Rnf12	ring finger protein 12	transcription /// ubiquitin cycle /// metal ion binding
Rnf128	ring finger protein 128	proteolysis /// ubiquitin cycle /// negative regulation of cytokine biosynthetic process /// metal ion binding
Tbl1xr1	transducin (beta)-like 1X-linked receptor 1	transcription /// ubiquitin cycle /// signal transduction /// chromatin modification /// GTPase activity
Tceb1	transcription elongation factor B (SIII), polypeptide 1	transcription /// ubiquitin cycle /// protein binding
Trim63	tripartite motif-containing 63	ubiquitin cycle /// muscle contraction /// proteasomal ubiquitin-dependent protein catabolic process /// metal ion binding
Ube2e3	ubiquitin-conjugating enzyme E2E 3, UBC4/5 homolog (yeast)	regulation of cell growth /// protein modification process /// ubiquitin-dependent protein catabolic process /// ubiquitin cycle
Mitochondrion, ER, Golgi		
Trp53	transformation related protein 53	protein import into nucleus, translocation /// regulation of progression through cell cycle /// transcription /// induction of apoptosis /// response to DNA damage stimulus /// ER overload response /// cell cycle /// caspase activation via cytochrome c /// positive regulation of transcription from RNA polymerase II promoter /// negative regulation of fibroblast proliferation
Abcb7	ATP-binding cassette, sub-family B (MDR/TAP), member 7	transport /// ATPase activity /// ATP binding /// nucleotide binding /// mitochondrial inner membrane
Bbc3	Bcl-2 binding component 3	release of cytochrome c from mitochondria /// induction of apoptosis /// caspase activation /// negative regulation of cell growth /// DNA damage response, signal transduction by p53 class mediator resulting in induction of apoptosis /// mitochonrial envelope
Gad1	glutamic acid decarboxylase 1	synaptic transmission /// carboxylic acid metabolic process /// neurotransmitter biosynthetic process /// mitochondrion
Agpat2	1-acylglycerol-3-phosphate O-acyltransferase 2 (lysophosphatidic acid acyltransferase, beta)	metabolic process /// phospholipid biosynthetic process /// 1-acylglycerol-3-phosphate O-acyltransferase activity /// ER /// integral to membrane
Asah3l	N-acylsphingosine amidohydrolase 3-like	lipid metabolic process /// ceramide metabolic process /// Golgi membrane /// ER membrane
Cds1	CDP-diacylglycerol synthase 1	phospholipid biosynthetic process /// CDP-diacylglycerol biosynthetic process /// phosphatidate cytidylyltransferase activity /// magnesium binding /// ER membrane

Cyp1a1	cytochrome P450, family 1, subfamily a, polypeptide 1	electron transport /// monooxigenase activity /// iron ion binding /// extracellular space /// ER /// microsome
Cyp1b1	cytochrome P450, family 1, subfamily b, polypeptide 1	electron transport /// monooxigenase activity /// iron ion binding /// extracellular space /// ER /// microsome
Cyp2s1	cytochrome P450, family 2, subfamily s, polypeptide 1	electron transport /// monooxigenase activity /// iron ion binding /// extracellular space /// ER /// microsome
Fvt1	follicular lymphoma variant translocation 1	metabolic process /// oxidoreductase activity /// ER /// integral to membrane
Lrpap1	low density lipoprotein receptor-related protein associated protein 1	receptor activity /// heparin binding /// low-density lipoprotein receptor binding /// ER /// plasma membrane
Tmc6	transmembrane channel-like gene family 6	transpor /// transporter activity /// ER /// integral to membrane
Gnpnat1	glucosamine-phosphate N-acetyltransferase 1	UDP-N-acetylglucosamine biosynthetic process /// glucosamine 6-phosphate N-acetyltransferase activity /// N-acetyltransferase activity /// late endosome /// ER-Golgi intermediate compartment
Optn	optineurin	protein targeting to Golgi /// Golgi organization and biogenesis /// biological_process /// Golgi to plasma membrane protein transport /// Golgi apparatus
Sgms2	sphingomyelin synthase 2	lipid metabolic process /// sphingolipid metabolic process /// sphingomyelin biosynthetic process /// kinase activity /// transferase activity /// Golgi apparatus
St6gal1	beta galactoside alpha 2,6 sialyltransferase 1	protein amino acid glycosylation /// transferase activity /// integral to Golgi membrane
St8sia1	ST8 alpha-N-acetyl-neuraminide alpha-2,8-sialyltransferase 1	protein amino acid glycosylation /// positive regulation of cell proliferation /// transferase activity /// integral to Golgi membrane
Chic2	cysteine-rich hydrophobic domain 2	Golgi to plasma membrane transport /// Golgi-associated vescicles /// Golgi apparatus
Cytokine & Chemokine		
Klf6	Kruppel-like factor 6	transcription /// cytokine and chemokine mediated signaling pathway /// metal ion binding /// nucleus
Ltb	lymphotoxin B	immune response /// lymph node development /// cytokine activity /// tumor necrosis factor receptor binding /// plasma membrane
Nodal	nodal	in utero embryonic development /// transforming growth factor beta receptor signaling pathway /// multicellular organismal development /// positive regulation of cell proliferation /// cell migration /// stem cell maintenance /// cytokines activity /// extracellular scape
Socs2	suppressor of cytokine signaling 2	regulation of cell growth /// intracellular signaling cascade /// negative regulation of signal transduction /// growth hormone receptor binding /// insuline-like growth factor receptor binding
Socs3	suppressor of cytokine signaling 3	regulation of cell growth /// regulation of protein amino acid phosphorylation /// intracellular signaling cascade /// negative regulation of signal transduction /// negative regulation of insulin receptor signaling pathway
Zc3h15	Zinc finger CCCH-type containing 15	cytokine and chemokine mediated signaling pathway
Bmp4	bone morphogenetic protein 4	skeletal development /// positive regulation of protein amino acid phosphorylation /// multicellular organismal development /// BMP signaling pathway /// positive regulation of cell differentiation /// cytokine activity /// growth factor activity /// heparin binding
Ccl25	chemokine (C-C motif) ligand 25	chemotaxis /// chemotaxis /// inflammatory response /// immune response /// signal transduction /// leukocyte migration /// cytokine and chemonine activity
Cxcl16	chemokine (C-X-C motif) ligand 16	chemotaxis /// immune response /// low-density lipoprotein receptor activity /// scavenger receptor activity /// cytokine activity /// chemokine activity
Cytoskeleton		
Cdc42ep3	CDC42 effector protein (Rho GTPase binding) 3	regulation of cell shape /// actin cytoskeleton
Ctnna1	catenin (cadherin associated protein), alpha 1	cell adhesion /// establishment and/or maintenance of cell polarity /// negative regulation of apoptosis /// positive regulation of smoothened signaling pathway /// cadherin binding /// actin filament binding /// adherens junction /// lamellipodium /// zonula lamellipodium
Dsg2	desmoglein 2	cell adhesion /// homophilic cell adhesion /// calcium ion binding /// integral ot membrane /// desmosome
Epb4.9	erythrocyte protein band 4.9	cytoskeleton organization and biogenesis /// barbed-end actin filament capping /// actin binding

Flnb	filamin, beta	striated muscle development /// actin binding /// stress fiber cytoplasm /// focal adhesion /// cytoskeleton
Frmd4a	FERM domain containing 4A	binding /// cytoskeleton
Gphn	gephyrin	protein targeting /// Mo-molybdopterin cofactor biosynthetic process /// establishment of synaptic specificity at neuromuscular junction /// catalytic activity /// cytoskeletal protein binding
Kras	v-Ki-ras2 Kirsten rat sarcoma viral oncogene homolog	regulation of progression through cell cycle /// small GTPase mediated signal transduction /// Ras protein signal transduction /// positive regulation of cell proliferation /// actin cytoskeleton organization and biogenesis /// regulation of synaptic transmission, GABAergic /// positive regulation of Rac protein signal transduction ///
Mtss1	metastasis suppressor 1	cell motility /// actin filament organization /// cell adhesion /// signal transduction /// transmembrane receptor protein tyrosine kinase signaling pathway /// actin filament polymerization /// filopodium formation /// actin binding /// ruffle /// andocytic vescicle
Synpo2l	synaptopodin 2-like	actin binding /// protein binding /// cytoskeleton
Ttl	tubulin tyrosine ligase	microtubule cytoskeleton organization and biogenesis /// protein modification process /// regulation of axon extension /// tubulin-tyrosin ligase activity /// magnesium-potassium ion binding /// microtubule
Arhgap8	Rho GTPase activating protein 8	actin cytoskeleton organization and biogenesis /// positive regulation of cell migration /// GTPase activator activity
Immune-Response and General Interest		
Relb	avian reticuloendotheliosis viral (v-rel) oncogene related B	regulation of progression through cell cycle /// transcription /// cellular process /// antigen processing and presentation /// T-helper 1 type immune response /// myeloid dendritic cell differentiation /// T-helper 1 cell differentiation /// regulation of transcription
Arl6ip2	ADP-ribosylation factor-like 6 interacting protein 2	immune response /// nucleotide response /// GTPase activity
Cd55	CD55 antigen	immune response /// complement activation, classical pathway /// innate immune response /// GPI anchor binding
Eif2ak2	eukaryotic translation initiation factor 2-alpha kinase 2	translation /// protein amino acid phosphorylation /// immune response /// response to virus /// unfolded protein response /// protein amino acid autophosphorylation /// RNA binding /// transferase binding /// protein kinase activity /// protein serine/threonine kinase activity
Centd3	centaurin, delta 3	signal transduction /// regulation of cell shape /// negative regulation of cell migration /// negative regulation of Rac protein signal transduction /// negative regulation of Rho protein signal transduction /// regulation of GTPase activity /// ruffle /// lamellipodium /// Rho GTPase activator activity
Gpr160	G protein-coupled receptor 160	signal transduction /// G-protein coupled receptor protein signaling pathway /// rhodopsin-like receptor activity
Gpr83	G protein-coupled receptor 83	signal transduction /// G-protein coupled receptor protein signaling pathway /// rhodopsin-like receptor activity
Mcf2l	mcf.2 transforming sequence-like	intracellular signaling cascade /// Rho protein signal transduction /// regulation of Rho protein signal transduction /// lamellipodia
Tbc1d24	TBC1 domain family, member 24	regulation of Rab GTPase activity
Tbc1d9	TBC1 domain family, member 9	regulation of Rab GTPase activity /// GTPase activator activity
Kbtbd8	Kelch repeat and BTB (POZ) domain containing 8	intracellular protein transport /// exocytosis /// biological_process /// regulation of calcium ion-dependent exocytosis /// glucose homeostasis /// negative regulation of G-protein coupled receptor protein signaling pathway /// Rab GTOase binding
Rab11fip2	RAB11 family interacting protein 2 (class I)	///
Rims2	regulating synaptic membrane exocytosis 2	transport /// intracellular protein transport /// exocytosis /// intracellular signaling cascade /// calcium ion-dependent exocytosis /// cAMP-mediated signaling /// insulin secretion /// Rab GTPase binding

4.3.4.3.2 Functional category analysis using FatiGO on ASCA results

One of the problems related to functional genomics is the description of biological properties, functions and interactions shared by a set of genes. An answer to this problem is Gene Ontology that extracts information from scientific journals and provides a structured description of biological functions dividing them into molecular functions, biological processes and cellular components (Ashburner *et al.*, 2000). FatiGO is a web-based application [http://fatigo.bioinfo.cnio.es] able to extract relevant GO terms for a group of genes with respect to a set of reference genes. FatiGO is used here to investigate which functional categories are over- or under-represented in the two groups of genes up-regulated and down-regulated obtained from ASCA analysis compared to the entire list of genes on the microarray chip. FatiGO extracts the function category from GO once the level at which the statistical contrast is going to be performed is indicated. Usually level 3 is used but lower terms in GO hierarchy are more precise. Also FatiGO returns adjusted p-values based on three different ways of accounting for multiple testing (Al-Shahrour *et al.*, 2004). The analysis was performed to determine the functional categories of cellular–component, molecular-function, biological process and pathway reported in KEGG (Kyoto Encyclopedia of Genes and Genomes), and the results are reported in Tables 4.16 and 4.17 for up- and down-regulated genes, respectively.

Table 4.16 FatiGO analysis of up-regulated genes from ASCA analysis

The list of up-regulated genes was analyzed for Functional Category enrichment with FatiGO and the results are reported here. Among the genes up-regulated, enrichment of four categories was identified but no pathway was statistically significant.

ASCA analysis up-regulated genes				
Biological process	**Level**	**n of genes**	**Unadj. p-value**	**Adj. p-value**
response to unfolded protein	5	5	0.000006	0.017700
macromolecule metabolic process	3	37	0.000010	0.020200
primary metabolic process	3	39	0.000037	0.047000

Cellular component	**Level**	**n of genes**	**Unadj. p-value**	**Adj. p-value**
Nucleus	8	31	0.000013	0.020600

Table 4.17 FatiGO analysis of down-regulated genes from ASCA analysis

The list of down-regulated genes was analyzed for Functional Category enrichment with FatiGO and the results are reported here. Among the genes down-regulated, enrichments can be observed in the TGF-β signaling pathway, and predominantly in transcription or DNA binding proteins.

ASCA down-regulated genes analyzed with FatiGO				
KEGG	**Genes list**	**Number of Genes**	**Unadj. p-value**	**Adj. p-value**
TGF-beta signaling pathway	Id3, Fst, Nodal, Id2, Bmp4, Id1	6	0	0.0096

Cellular components	**Level**	**Number of Genes**	**Unadj. p-value**	**Adj. p-value**
nucleus	8	34	0.0004	0.0825

Biological process	**Level**	**number of genes**	**Unadj. p-value**	**Adj. p-value**
multicellular organismal development	3	25	0	0.0115
anatomical structure development	3	22	0.0001	0.0462
negative regulation of transcription	8	9	0	0.0221
regulation of transcription, DNA-dependent	8	26	0.0001	0.0434
negative regulation of transcription factor activity	9	3	0	0.0115

Cellular functions	**Level**	**Number of Genes**	**Unadj. p-value**	**Adj. p-value**
nucleic acid binding	3	29	0.0002	0.0541
transcriptional repressor activity	3	6	0.0002	0.0602
nucleotide binding	3	1	0.0003	0.0688
DNA binding	4	23	0	0.0096
unspecific monooxygenase activity	6	3	0.0003	0.0688

4.3.4.3.3 Real Time RT-PCR relative quantification on genes derived from ASCA analysis

ASCA analysis does not provide the fold change in expression so it is difficult to confirm this data by real time RT-PCR. However RT-PCR can give a confirmation of the expression trend of a gene during infection. For this reason, total RNA extracted at 2 and 4 hours post-infection were employed in this experiment as well as appropriate control RNA populations. The genes were chosen for their potential relevance to host-pathogen interaction studies. In addition, a few genes that were identified in previous analyses described in this thesis were included. These were Lamp2 and Socs3, already shown to be down- and up-regulated during ES cell infection. Other genes included examples involved in the regulation of apoptosis, cytosckeleton rearrangement and a TGF-β binding protein. For a more detailed description of each gene please refer to Table 4.14 and 4.15. The data are reported here as $ln2^{-\Delta\Delta Ct}$ that rapresents the ratio between the expression level of the target gene and the control gene (β-actin) expressed in ln scale (Figure 4.11).

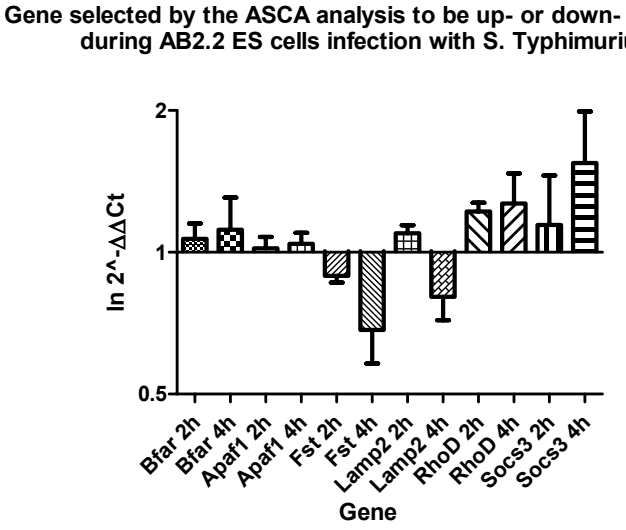

Figure 4.11 Real time RT-PCR relative quantification on ASCA analysis

A few genes selected by ASCA analysis to be positively or negatively regulated in murine ES cells AB2.2 during *S.* Typhimurium infection were chosen to perform relative quantification by real time RT-PCR. In this analysis the Ct values of target genes were compared to the Ct value of an internal control β-actin and the ratios were calculated and plotted as $ln\ 2^{-\Delta\Delta Ct}$. The reactions were carried out in triplicate for each biological replicate at 0h, 2h and 4h infection and the mean values are reported here. The error bars represent the standard error for each replicate.

RT-PCR was performed in order to confirm the results obtained by bioinformatics analysis of up- or down-regulated genes. In this case the genes to be confirmed by RT-PCR were chosen as they seemed relevant to this study. The RT-PCR results partially confirmed that those genes reported to be up- or down-regulated by bioinformatics analysis were in fact up- or down-regulated. The Socs3 gene, however, was reported to be down-regulated by ASCA analysis, whereas it was up-regulated in the other analysis as also confirmed by RT-PCR. Refer to Appendix A for a short description of the genes used in this experiment.

4.3.4.3.4 Statistical analysis of RT-PCR data on genes identified by ASCA

Statistical analysis was performed on the real time RT-PCR Ct values obtained on a few genes identified by ASCA analysis. The analysis was performed comparing the expression leves at 4 hours post-infection to the uninfected cells since there were larger expression difference between these samples. The statistical analysis was conducted using REST© 2005. The results form this analysis are shown in Figure 4.12 as a graph plotting the expression range for each gene. This analysis reported no significant difference in the expression levels of the genes taken into consideration here.

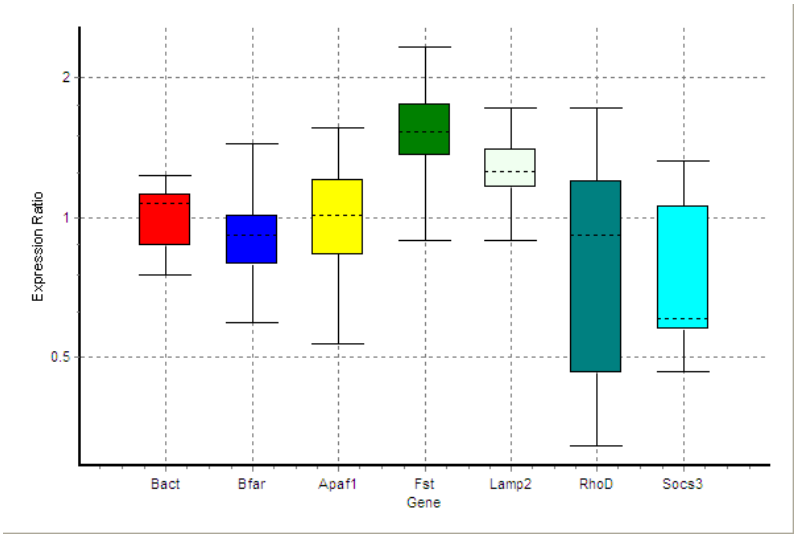

Figure 4.12 Whisker box of the RT-PCR analysis on genes identified by ASCA

The statistical analysis of the Ct values determined from the RT-PCR analysis is here represented as whisker boxes representing the mean value of three independent reactions for each gene. The statistical analysis did not indentified any statistically significant difference between the mean Ct values of the target genes compared to the mean Ct value of the control gene β-actin.

4.4 Discussion

This chapter reports the results from the transcription profile of AB2.2 murine ES cells during infection with *S.* Typhimurium SL1344. The concept behind these experiments was to investigate whether ES cells could be developed as a novel *in vitro* model by which to study the response of eukaryotic cells to bacterial infection. It is now well established that microarrays can be used to monitor how immunological cells subjected to bacterial invasion respond in terms of gene expression patterns (Detweiler *et al.*, 2001; Rosenberger *et al.*, 2000). Further work has also been reported on infected epithelial cells that can respond by producing cytokines and other immune factors (Eckmann *et al.*, 2000). Two factors should be kept in mind in the interpretation of the data presented here. Firstly, at least 30% of the cells were infected at 2 hours and 4 hours post-infection. The percentage of cells infected will inevitably have effects on the resulting p-values and fold expression. However it has not been common practise in published papers reporting transcription profile during bacterial infection, to include data on percentage of infected cells. The second factor to consider is that, as noted in previous publications, the response of differentiated cells to pathogen invasion overwhelmingly involves genes linked to the immune response. Interestingly, in the ES cell model used here, this response was not observed and it is possible that by using murine ES cells, that lack a strong immune signature, to highlight other components involved in alternative cellular reaction to pathogen invasion.

Pathogens are able to manipulate host components to their advantage. For example, it has previously been described how *Salmonella* secretes SPI-1 TIIISS effector proteins inside non-phagocytic cells directing its own phagocytosis. The TIIISS are specialized protein structure with the ability to deliver a specific set of bacterial proteins into the host cells to modulate or interfere with cellular functions; this mechanism is essential for the virulence of many important bacteria such as *Salmonella*, *Shigella* and *Yersinia pestis* (Kubori & Galan, 2003). Also a second *Salmonella* TIIISS, harboured on the SPI-2 loci, injects proteins inside the host from the SCV. Examples of SPI-2 effectors include SifA which is involved in the maintenance and survival of the bacteria inside the host cells (Brumell *et al.*, 2002).

In the analysis reported here at least four important groups of genes can be distinguished that are apparently differentially regulated during bacterial infection. These include a limited number of immunological genes, genes involved in cell cycle regulation, many genes involved in stress response, associated with ER and protein folding, and components of the mitochondrion. Finally the expression of several transcription factors is affected. Hereafter, I will talk briefly about some genes that are included in these categories.

Among the genes involved in the cell cycle regulation one that comes up as strongly up-regulated in all the analyses is *Banp*, Btg3 associated nuclear protein. This is part of the BTG family of proteins, of which several members play a role in the negative control of the cell cycle. It was reported that BTG3 is induced by redox changes, with RNA levels peaking at the end of G1 phase of the cell cycle (Birot *et al.*, 2000). In other studies investigating host-pathogen response BTG1 was reported to be up-regulated in swine lymph nodes after infection with *S.* Choleraesuis (Uthe *et al.*, 2007) and in human epithelial cells infected with *S.* Dublin (Eckmann *et al.*, 2000).

Genes involved in ubiquitination were also identified as differentially expressed in this experiment. Ubiquitination can have an important role in bacterial infection, for example *Pseudomonas aeruginosa* (Balachandran *et al.*, 2007). In this study, the 'ubiquitin mediated proteolysis' pathway was determined to be differentially up-regulated by InnateDB analysis (Table 4.6). In the ASCA time course analysis seven genes involved in the ubiquitin cycle were also identified as up-regulated (Table 4.14) and ten were apparently attenuated during infection (Table 4.15). Ubiquitination is the main protein degradation pathway that governs a variety of cellular processes including cell cycle, vesicle trafficking and signal transduction. Bonifacino and Weissman (1998) report an exhaustive review on ubiquitins and their role in the immune system (Bonifacino & Weissman, 1998). During *Salmonella* invasion at least one protein secreted inside host cells by SPI-1, SopE, is an object of ubiquitination and rapid degradation soon after injection (Kubori & Galan, 2003). SopA can also serve as a substrate for HsRMA1-mediated ubiquitination. In this case though, it was speculated that mono- or poly-ubiquitination can modulate the protein activity and *Salmonella* SCV escape inside the host cells (Zhang *et al.*, 2005). However, the first *Salmonella* protein to be described to be ubiquitinated, once inside the host cell, was a SIP-1

secreted protein, SopB. Although the authors did not observe a rapid degradation by the proteasome thereafter, they hypothesized that the ubiquitination would regulate SopB activity and attenuate cyto-toxicity (Marcus *et al.*, 2002). In fact it was reported that ubiquitination not only has a role in protein metabolism but in particular mono-ubiquitination is a regulator of the location and activity of diverse cellular proteins (Hicke, 2001). The gene involved in ubiquitination with the highest differential expression during infection of murine ES cells was *Herpud1*. The homocystein-inducible, endoplasmic reticulum stress-inducible, ubiquitin-like domain member 1 (Herpud1), was reported to be involved in the ER-stress response where it is a resident-chaperone protein. Herpud1 was originally described as the first integral membrane protein regulated by the ER stress response pathway and was suggested to play an unknown role in the cellular survival response to stress in the unfolded protein response (UPR) (Kokame *et al.*, 2000).

The ER stress response can also activate another cellular signalling pathway named EOR (ER overloaded response); this is activated by the accumulation of membrane proteins in the ER and is distinct from the signalling induced by UPR. The EOR signalling pathway activates nuclear factor (NF)-κB which then induces the transcription of pro-inflammatory and immune response genes. GeneSpring analysis revealed the up-regulation of *NFκbiz* (nuclear factor kappa light chain polypeptide gene enhancer in B-cell, inhibitor zeta) (Table 4.10) and ASCA analysis reported the down-regulation of *NFκbia* (nuclear factor kappa light chain polypeptide gene enhancer in B-cell, inhibitor alpha) (Table 4.15). *NFκbiz* gene is a member of the ankyrin-repeat family with high sequence similarity to the C-terminal of IκB proteins. Bioconductor analysis also revealed mRNA encoding for the ankyrin-repeat member 37 to be up-regulated (Table 4.3, Table 4.4), reported also in GeneSpring analysis (Table 4.12). The transcription factor NF-κB plays a crucial role in a wide variety of cellular functions and its activity is strictly regulated by cytosolic inhibitors known as IκBs. IκB is induced by lipopolysaccharide (LPS) or IL-1β and is localized in the nucleus where it is thought to bind NF-κB thus preventing an excessive inflammatory response. Also, NFκbiz supports the regulation of a subset of inflammatory genes represented by IL-6, it inhibits the expression of TNF-α and is reported to promote TNF-α-induced apoptosis (Yamazaki *et al.*, 2001). NFκbia is reported to play a role in viral infection (Hiscott *et*

al., 1997). The regulation of NFκB is complex and this transcription factor itself regulates the expression of many cellular biological functions including inflammation, stress and immune responses, embryonic development and apoptosis (Liu-Mares *et al.*, 2007).

Microarray analysis also identified a few transcription factors as being differentially expressed during *Salmonella* infection. Two transcription factors whose expression was significantly induced during bacterial infection were *eIf2ak2* and *3* (eukaryotic initiation factor 2 alpha, kinase 2 and 3). They were identified during both GeneSpring and ASCA analysis (Tables 4.11 and 4.14). The phosphorylation of this class of proteins immediately inhibits additional translational initiation events (Kaufman, 1999). The time course analysis revealed that *eIf2ak2*, also described as IFN-type I-induced and ds-RNA activated kinase, was down regulated during infection (Table 4.15).

Another transcription factor displaying a strong signal of differential expression in this study is XBP-1 (X-box binding protein-1). This transcription factor is essential for the differentiation of plasma cells and the UPR activation. This gene was also reported to be positively expressed in another publication detailing human macrophage-pathogen interactions (Nau *et al.*, 2002). In 2003 Iwakoshi *et al.* concluded that XBP-1 is absolutely required for plasma cell differentiation (Iwakoshi *et al.*, 2003). The same authors in 2007 reported that XBP-1 is necessary for maintaining ER homeostasis and preventing activation of cell death pathways caused by sustained ER stress. Also they reported that *XBP-1* expression is essential for dendritic cell development and survival, which confirms its importance in the differentiation of highly secretory cells like embryonic hepatocytes, exocrine pancreatic acinar cells and plasma cells (Iwakoshi *et al.*, 2007).

Among the genes involved in the mitochondrion homeostasis, monooxygenease genes such as cytochrome P450a and b were strongly down-regulated at 4 hours post-infection with *S.* Typhimurium (Table 4.3, 4.4, 4.11, 4.12, 4.15) although they were first up-regulated at 2 hours post-infection (Table 4.2 and 4.10). The alteration of the expression of the oxidoreductase genes was reported in other studies investigating the host response to pathogens (Handley & Miller, 2007; Rosenberger *et al.*, 2001). The smooth ER expands as the enzymes that oxidize and detoxify are induced to meet their demand

and the overproduction of recombinant *Candida maltosa* P450Alk1 in *S. cerevisiae* activates the UPR to proliferate the ER extensively (Kaufman, 1999). It was proposed that the P-450 down-regulation is a pathophysiological effect of the inflammation progression, a scheme of which is reported in Figure 4.13 (Morgan, 2001).

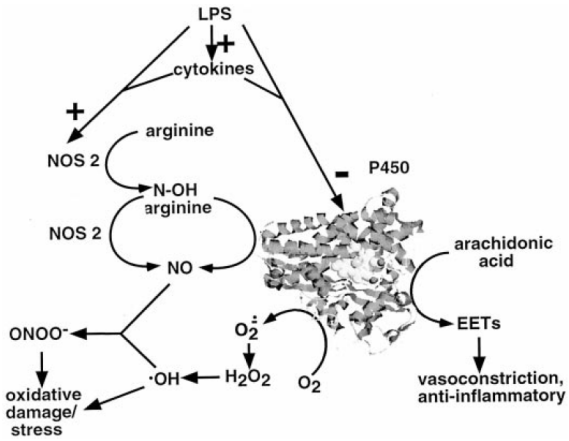

Figure 4.13 Supposed regulation of P450 cytocrome during cellular response to inflammation (Morgan, 2001)

Pathway analysis conducted with InnateDB did not reveal any significantly (for adjusted p-value) up-regulated (Table 4.5, 4.6, 4.8) or down-regulated pathways (Table 4.7, 4.9). However among the potentially up-regulated pathways identified, a few were quite interesting and they highlight how *Salmonella* invasion may interfere with lipid synthesis, ER trafficking and cell motility signalling pathways (Table 4.6).

Among these, the ERAD pathway or ER-associated degradation pathway is involved in the cytosolic degradation of misfolded proteins present in the ER. Once in the cytosol the proteins are deglycosylated, ubiquitinylated and directed to proteasome degradation (Tsai *et al.*, 2002). It has been observed that ERAD can be subverted by viral infection to trigger MHC class I breakdown (Tortorella *et al.*, 2000). It is also possible that bacterial invasion triggers the ER stress response similar to that for viral infection, depicted in Figure 4.14 (Medigeshi *et al.*, 2007). This response may also be a defense mechanism since, under conditions of severe ER stress, eukaryotic cells generate a signal that induces programmed cell death known as apoptosis. However, the molecular signalling mechanisms that link ER stress to downstream caspase activation resulting in cell death remain largely unknown (Kaufman, 1999).

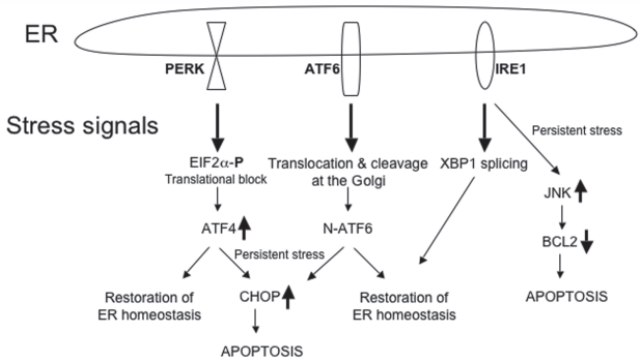

Figure 4.14 ER stress response to viral infection (Medigeshi et al., 2007)

The stringency of statistical analysis often does not accomodate the flexibility and variability of biological systems very well. In this study the data analysis using GeneSpring software revealed more interesting and previously reported genes implicated in host-bacteria interactions. For example among the positively regulated genes can be recognized *Socs* (suppressor of cytokine signalling) (Dalpke *et al.*, 2008), *Stat2* (involved in the transduction and transcription of type I interferon signalling), *Lyst*, (lysosomal trafficking regulator) and *clk2* (CDC-like kinase 2) all of which were previously described to be somehow involved with the pathogen interaction.

This study reported that several genes of murine ES cells were significantly differentially expressed during *S.* Typhimurium invasion, however a few of these are known to be involved in immunological responses. Most of the genes reported are principally involved in the cellular reaction to bacterial invasion. Few of them have been documented in previous host-pathogen transcription profile studies but perhaps they were not discussed because they were not thought relevant to the immune response. Sometimes the interpretation of microarray data can be distorted by the expectations and previous observations of the system studied.

The use of whole genome arrays gives the researcher new insight into host-pathogen interactions that can potentially lead to the discovery of new pathways likely to be promising as new drug targets. However, only their combined use with sequence information, computational tools and the traditional approaches of biology, biochemistry, chemistry, physics, mathematics and genetics can increase the hope of

understanding the function and the regulation of all genes and proteins (Lockhart & Winzeler, 2000).

5 Procedures for differentiating mouse Embryonic Stem cells into dendritic cell

5.1 Introduction

5.1.1 Stem cells and *in vitro* differentiation

A hallmark and defining property of stem cells is their capacity for self-renewal and differentiation. The science of stem cell biology is still young and the properties of these cells have not been fully explored and there is more to be discovered in terms of research and their potential therapeutic applications. Few stem cells types have been characterised and described since their discovery in the early 1980s. Denham and co-workers distinguished five types of stem cells: unipotent stem cells, which are a type of cell that undergoes self-renewal and gives rise to only one mature cell type; multipotent stem cells that are characterized by the ability to undergo self-renewal and have the capacity to yield at least two differential foetal or adult cell types; pluripotent stem cells, which are capable of self-renewal and give rise to a vast array of mature cell types; totipotent stem cells, which replicate and generate all adult and extraembryonic tissues of their species but undergo limited self-renewal. The final type of stem cells are cancer stem cells, which replicate and undergo self-renewal but their compromised self-renewal pathway results in neoplasia (Denham *et al.*, 2005).

Pluripotent stem cells are heavily utilized in research and these cells are currently favoured for the exploitation of their therapeutic potential. *In vitro*-generated embryonic germ (EG) cells, embryonal carcinoma (EC) cells and embryonic stem (ES) cells can be generated from this type of stem cell. ES cells originate from the inner cell mass of an embryo at the blastocyst developmental stage, and thus they theoretically possess the capacity to give rise to every cell type of the adult organism. This quality of pluripotent stem cells has already been largely demonstrated. ES cells have the ability to provide replacement tissue or they can be used as a means to understand disease mechanisms. Before these goals can be routinely and rationally achieved, the precise methods of how to differentiate stem cells into exactly the right lineage, in a homogenous or near-

homogenous form needs to be addressed. Also other areas where progress still has to be made include the ethics of their use, the suppression of immune rejection and the accessibility of sites within the patient (Denham *et al.*, 2005).

Mouse ES cells are nowadays the best characterized stem cells lines and they have already been driven to differentiate *in vitro* into diverse cell lineages such as cardiac muscle, neural crest, neural stem and haematopoietic lineages, just to mention a few. It is believed, or hoped, that human ES cells may eventually be driven *in vitro* to differentiate into any desired cell of the body for potential use therapeutically (Denham *et al.*, 2005). The first reports of the *in vitro* differentiation of ES cells into haematopoietic lineages came in 1991 using direct differentiation from *in vitro* grown ES cells. Wiles and colleagues (1991) reported the differentiation of four haematopoietic lineages from embryoid bodies: erythroid cells, macrophages, neutrophils and mast cells. In their publication, Wiles and colleagues commented with enthusiasm and a little surprise about the consistency and the large number of cells produced by their method (Wiles & Keller, 1991). Moreover the practical exploitation of differentiated antigen presenting cells (APC) deriving from ES cells was reported by Moore *et al.* in 1998. Here *in vitro* ES cells differentiated into macrophages were used in a study on atherosclerosis. In addition, these authors reported the use of transfected ES cells (Moore *et al.*, 1998). They recognized the advantage of using ES cells differentiated into APC resides in the fact that genetic manipulations can be performed on primary stem cells prior to differentiation. Schmitt *et al.* (2004) reported the possibility of differentiating ES cells into mature and functioning T cells. They successfully reconstituted the T cell compartment of immunodeficient mice using differentiated stem cells, enabling an effective response to a viral infection (Schmitt *et al.*, 2004).

The potential of murine ES cells to be differentiated into dendritic cells (DCs) with the ability to present antigen to naïve T cells was explored in order to further investigate the potential application of stem cells to infectious diseases studies.

5.1.2 Dendritic cells and their *ex-vivo* extraction and research application

Dendritic cells are highly specialized APCs that perform a very important role in the immune system, which is to link innate and adaptive immune responses mediating T cell activation and antigen-specific responses. DCs together with macrophages are considered a primary target for initiating immune responses to infection and they play a central role in the body's fight against pathogens. DCs are sentinel cells that continuously sense the environment and coordinate defenses for the protection of mucosal tissues. Mucosal surfaces represent the main site of interaction with microorganisms and antigens from the external environment. Immature DCs are essential cells with phagocytic potential, resident in the sub-epithelial and intra-epithelial compartments of the mucosa. Here, DCs play an active role in bacterial uptake by sampleing the lumen content. This is possible because DCs are able to open the tight junctions cottecting epithelia cells (Rimoldi *et al.*, 2004). Upon maturation, normally induced by either pathogen-associated molecular patterns or microorganisms, DCs function as APCs and commonly migrate into mucosal-associated lymph nodes to initiate adaptive immunity (Niedergang *et al.*, 2004). Some researchers believe that a major "bottleneck" in mucosal DC research is the difficulty to isolate DCs without altering their phenotype. This is one of the reasons that the application of ES in the *in vitro* differentiation of DCs could have a great impact in mucosal and pathogen-host interaction research. Usually DCs are isolated from *ex-vivo* tissue like spleen and blood in a post-mitotic form by flow cytometry or magnetic bead sorting, which can be rather inefficient and expensive when a small number of target cells are present in the sample. For example, myeloid DCs make up less then 1% of the mononuclear cells present in the peripheral blood (van Helden *et al.*, 2008). In addition the life span of such culture is limited since DCs obtained in this way are terminally differentiated and cannot divide. The source of the sample can also have an impact on the quality and the quantity of cells you can obtain from an *ex-vivo* model. Larger numbers of DCs can be obtained from bone marrow stem cells, peripheral blood mononuclear cells or monocytes (Inaba *et al.*, 1992). However, it is not possible to avoid variability in the source cell population and the consequent variability in the resulting DCs. The common downside in research on this type of cell is that transfection and electroporation with recombinant DNA or short hairpin RNAs is generally very ineffective and associated with significant cell death (van Helden *et al.*, 2008).

The results of attempts to *in vitro* differentiate AB2.2 murine ES cells into dendritic cells are reported in this chapter. A protocol published by Dr. Fairchild was employed (Fairchild *et al.*, 2000) for the first time in the laboratory of Professor Gordon Dougan and in other labs at the Sanger Institute. The ES cell derived dendritic cells (esDC) were characterized for surface marker expression by flow cytometric analysis and these were compared to bone marrow derived DCs (BMDC). Primary DCs were obtained as control from the bone marrow of 129/Sv mice. Here, the monocytes present in bone marrow were incubated *in vitro* with IL-4 and GM-CFS cytokines. The subsequent esDCs were further characterized by confocal and electron microscopy. Cytokine secretion was measured and antigen presentation assays were carried out to demonstrate the ability of esDCs to process and expose antigens to naïve T cells. These were successfully accomplished using ovalbumin (OVA) protein presented to T cells responding to species-specific OVA peptide.

5.2 Results

5.2.1 Formation of embryoid bodies and differentiation into dendritic cells

In order to differentiate murine ES cells into DCs, murine ES cells at a very low passage (nine passages) were employed. Early passage cells should guarantee the integrity of their karyotype and retain their full pluripotent ability to generate any kind of somatic cells. ES cells were donated by Professor Allan Bradley's laboratory, which also kindly supplied the irradiated feeder cells to maintain the primary ES cells in an undifferentiated state. Prior to differentiation ES cells were grown in feeder cell-free culture for 2 passages using gelatin treated culture flasks and the medium was enriched with 1000 U/ml of LIF to maintain the undifferentiated state. This procedure eliminated feeder cells that could interfere with the differentiation process and I was thus able to obtain a pure ES cell culture. The ES cells produced through this approach were then trypsinized and $4x10^5$ cells per Petri dish were grown in suspension in 20ml of LIF-free medium for 14 days. The cells were not able to adhere to the bacteriological plastic, which had not been treated with extracellular matrix proteins, and the absence of LIF allowed the single cells to replicate and form embryoid bodies (EBs). EBs are three dimensional structures in which the growing cells are differentiating spontaneously into many cell types including myeloid cells. EBs become macroscopic structures in 4-5 days and they can appear as a simple cluster of cells with no polarity or can become cystic, forming a large fluid-filled blister-like structure. Cells within either of those structures should maintain the ability to differentiate into DCs. Figure 5.1 shows an image of a cystic EB.

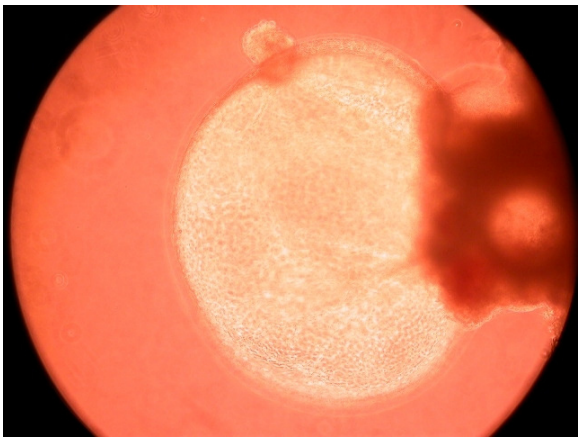

Figure 5.1 Image of a cystic EB

EBs were obtained from single ES cells growing in suspension in medium free of LIF. These culture conditions potentially permit the growth from a single cell to form a cluster of cells differentiating into any type of precursor cells. EBs can then be used to obtain differentiated cells via specific cytokines that drive the multipotent cells into a specific differentiation pathway.

Fourteen day old EBs were seeded into tissue culture dishes with selective medium containing 25ng/ml of mouse recombinant granulocyte-macrophage colony stimulating factor (GM-CSF) and 200 WHOSU/ml of recombinant IL-3. It is important that the EBs have enough space to adhere, grow and expand to produce DCs. For this reason about 10-15 EBs were seeded per 10cm tissue culture dish. After 48 hours of incubation the majority of EBs adhered to the culture plastic. At this stage many morphologically distinct cell types may be observed. For example, cardiomyocytes are normally easily distinguished. Cardiomyocytes develop spontaneously without the addition of external factors and their appearance is an indication of the 'good health' of the culture and their presence indicates that the EBs are following a normal differentiation program. Each culture can have a slightly different differentiation time, but it was possible to observe the first esDCs as early as 5 days after incubation with GM-CSF and IL-3. In these culture conditions differentiated cells with the features expected for DCs could be observed at the edge of an EB (Figure 5.2 panels 1 and 2). After a few more days of growth some esDCs were observed to relocate, forming little clusters of cells that subsequently became foci of replication for esDCs (Figure 5.2 panels 3 and 4). All these data correspond to and confirm the data published by Fairchild (Fairchild *et al.*, 2003), Figure 5.3 represents a schematic diagram of the process.

1

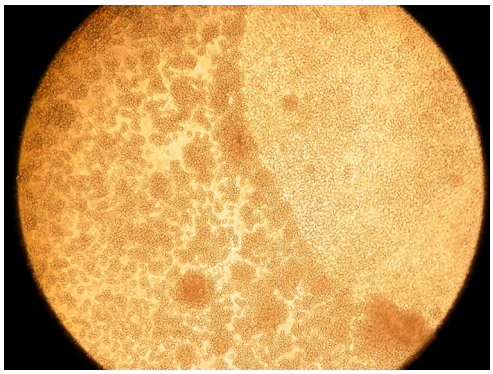

2

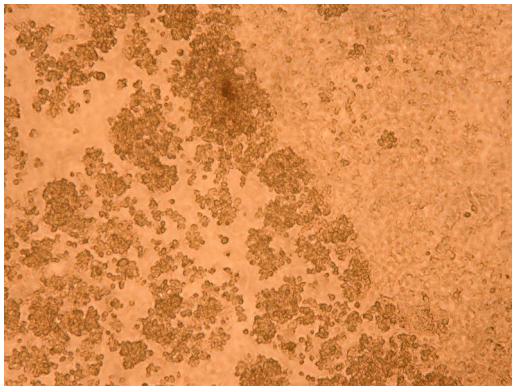

3

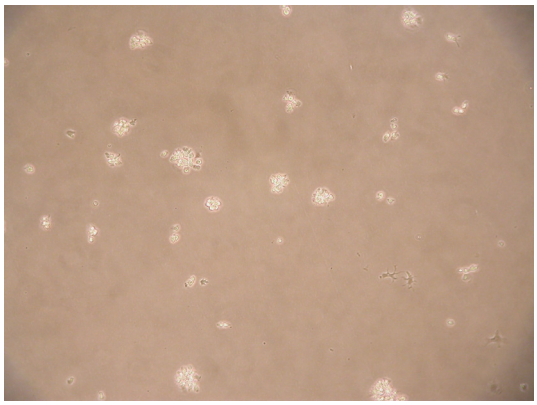

4

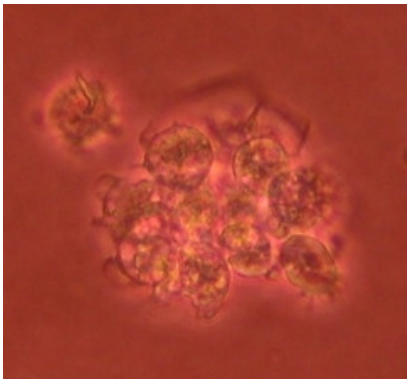

Figure 5.2 Images of esDCs emerging during differentiation from EBs

These optical microscopic images illustrate esDCs differentiating from EBs deriving from AB2.2 murine ES cells. Panel 1 shows the edge of an EB starting to 'produce' differentiated esDCs from the periphery. Clear morphological differences can be observed between the two types of cells. Particular features can be observed on panel 2. Panel 3 illustrates clusters of esDCs that are relocated outside the EB site and these will subsequently grow in proliferating foci of esDC. In panel 4 one can observe a cluster with cells bearing little protrusions. These are young esDCs.

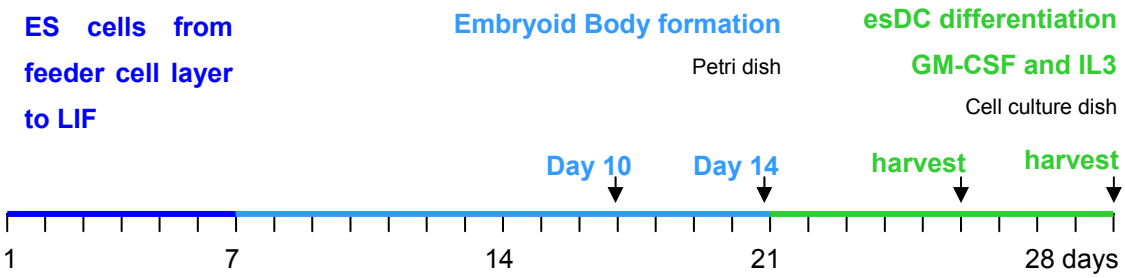

Figure 5.3 Scheme of the differentiation protocol for transforming murine ES cells into esDCs

The process was normally initiated using a new vial of cells each time but in a laboratory where the culturing of ES cells is routine and ongoing the first 7/10 days can be shortened. At the beginning of the project the ability to produce esDCs from EBs at different growth times (10 and 14 days) was investigated. Subsequently, the 14 day time point was favored. The esDCs can be harvested a few times from the same tissue culture dish, but a limiting factor is the culture surface and the ability to detach esDCs without dislocating EBs.

5.2.2 EsDC characterization by flow cytometric analysis

Murine esDCs were monitored for the expression of a number of surface markers characteristic of myeloid cells by flow cytometric analysis. Initially, surface markers similar to those used by Fairchild during the original characterisation of murine esDCs were employed (Fairchild *et al.*, 2003). Coloured beads were used to calculate the compensation parameters for overlapping fluorochrome, and unstained immature or mature cells were employed as negative controls as appropriate. The BMDCs, obtained from the same mouse allotype 129/Sv, were also employed as controls. The initial surface markers investigated included CD11b ($\alpha_M\beta_2$ integrin), also known as complement receptor 3 or CR3, which mediates adhesion to C3bi and ICAM-1 (CD54). CD11b is expressed at different levels on granulocytes, NK cells, macrophages, DCs and B-1 cells. CD11c expression was tested. CD11c it interacts with the integrin α-chain of gp150, which is expressed on DCs and at low levels on macrophages. To detect the expression of MHC class I and class II, anti-mouse H-$2K^b$ and anti-mouse I-A/I-E antibodies were employed respectively. Other markers tested were CD40, normally expressed on APC; CD44, widely expressed on haematopoietic cells and non-haematopoietic cells; CD45, reacting with the leukocyte common antigens (LCA) found on haematopoietic cells; CD54, also known as ICAM-1 a 95-kDa member of the Ig superfamily found on lymphocytes, macrophages and DC; CD80 (B7-1) also a member of the Ig superfamily that along with CD86 participates in the costimulation of T cells, CD80 constitutively expressed on DC, monocytes and peritoneal macrophages; CB86 (B7-2), a costimulatory molecule expressed on a broad spectrum of leukocytes with levels enhanced after antigen co-incubation; F4/80, a marker expressed on a wide range of mature macrophages and on a subpopulation of DC; CD205, also known as the dendritic and epithelial cell 205kDa antigen, which acts as an endocytic receptor expressed at high level on mouse DCs; Ly-6C or Gr-1, a characteristic marker of haematopoietic progenitors and granulocyte differentiation and maturation; DC-SIGN differentially expressed by sub-populations of DC and an antigen that may play a role in T cell-DC interaction. Additionally, TLR4, TLR2, TLR9 and TLR5 receptors were analyzed. This information was derived from the data sheet provided with each antibody.

Initially, the immature DCs were compared with mature DCs that were activated using the non-protein antigen *Salmonella* LPS at 10µg/ml a protein antigen ovalbumin (OVA) at 10µg/ml and TNFα at 5000WHOSU/ml, which are known to be able to activate DCs. LPS is a bacterial product reacting with TLR4 and has been described to activate DCs (Poltorak *et al.*, 1998). OVA is a non-TLR dependent antigen and needs to be actively phagocytosed by the cell and processed though the phagosome vesicle traffic system and then presented on the cell surface on MHC class I and II (Tangri *et al.*, 1998). TNFα is an inflammatory cytokine that strongly promotes the activation and maturation of DCs (Kikuchi *et al.*, 2003). However, TNFα was described to be able to semi-activate DC (Menges *et al.*, 2002). The activation and maturation of DCs is regulated by a variety of extracellular stimuli including cytokines, co-stimulatory molecules and bacterial products. These events induce profound alteration of the morphological, phenotypical and functional properties of DCs. The results from flow cytometric analysis are summarized in Table 5.1. The histograms resulting from these analyses and subsequently used to produce the table are reported in Appendix B.

Table 5.1 Flow cytometric analysis of surface markers of AB2.2 murine ES cells, esDC and BMDC, immature and matured with LPS, OVA and TNFα

This table summarizes the flow cytometric data obtained for surface markers detected on AB2.2 murine ES cells, esDCs and BMDCs either immature or incubated with LPS, OVA or TNFα. +/- indicates ~ 20% of the cells were positive, + indicates that at least 30% of the cells were positive, ++ indicates ~ 60% of the cells were positive, +++ indicates that ~ 90% of the cells were positive for the marker tested. All the cells were detached from the culture plastic using Cell Dissotiation buffer. N/A = not available.

* – indicates no difference with the isotype antibody control; + indicates a shift to the right of the peak specific for the taget marker. ** CD44 antibody proved later to have a high background.

Marker	AB2.2*	esDC	esDC LPS 24h	esDC TNFa 24h	esDC OVA 24h	BMDC	BMDC LPS 24h	BMDC TNFa 48h	BMDC OVA 24h
CD11b	-	++	+++	+++	++	++	++	+	++
CD11c	-	++	+++	+++	++	++	++	+	++
CD205	-	+	+	+	-	+	+	+	+/-
CD4	-	+	++	+	N/A	N/A	N/A	N/A	N/A
CD40	+	++	+++	++	+	++	++	+	+
CD44**	-	+++	+++	+++	+++	+++	+++	+++	+++
CD45	-	+++	+++	+++	+++	++	++	++	+++
CD54	+	++	+++	++	++	+	+	++	++
CD8	-	-	-/+	-	N/A	N/A	N/A	N/A	N/A
CD80	-	++	++	++	+++	-/+	+	+	++
CD86	-	-	-/+	-	-	-/+	+	-/+	+
DC-SIGN	+	+	++	+	N/A	+/-	-/+	-/+	-
F4/80	+	+++	+++	+++	+++	+++	+++	++	++
H-2K	-	+	++	+	+/-	++	+	+	+
IA/IE	-	-	-/+	-/+	-/+	+	++	+	++
TLR2	-	++	++	++	N/A	+	+	+	+
TLR4	-	+	++	+	++	+	-/+	+	+/-
TLR5	-	+	+	-/+	+	-/+	-	+/-	-
TLR9	-	+/-	+	-	N/A	N/A	N/A	N/A	N/A
Ly6C	N/A	-	+	N/A	N/A	-	-	-	-

5.2.3 Confocal characterization esDCs

The morphology and appearance of esDCs, immature and mature, was routinely investigated by light microscopy and typical images of these cells are shown in Figure 5.4 and 5.5. EsDCs showed long cellular protrusion, lamellipodia and filopodia as observed before in BMDCs. These cell populations were then further characterized for MHC II expression by fluorescent antibody coupled with confocal microscopy. Such cells were grown on coverslips pre-treated with poly-L-lysine and seeded at 2 $x10^5$ cells per well in 24 well plates. After 24 hours culture they were fixed with 1% paraformaldehyde and stained with rat anti-mouse MHC II antibody and finally mounted on a cover slip holder. Immature esDCs were permeabilised by exposure to saponin buffer in order to stain internal MHC class II (Figure 5.4). Mature esDCs were treated overnight with TNFα or LPS and were stained for surface expression of MHC class II using non-permeabilised cells (Figure 5.5). Mature esDCs clearly change morphology and strongly adhere to plastic. This experiment indicates that these cells may exist as immature and mature forms.

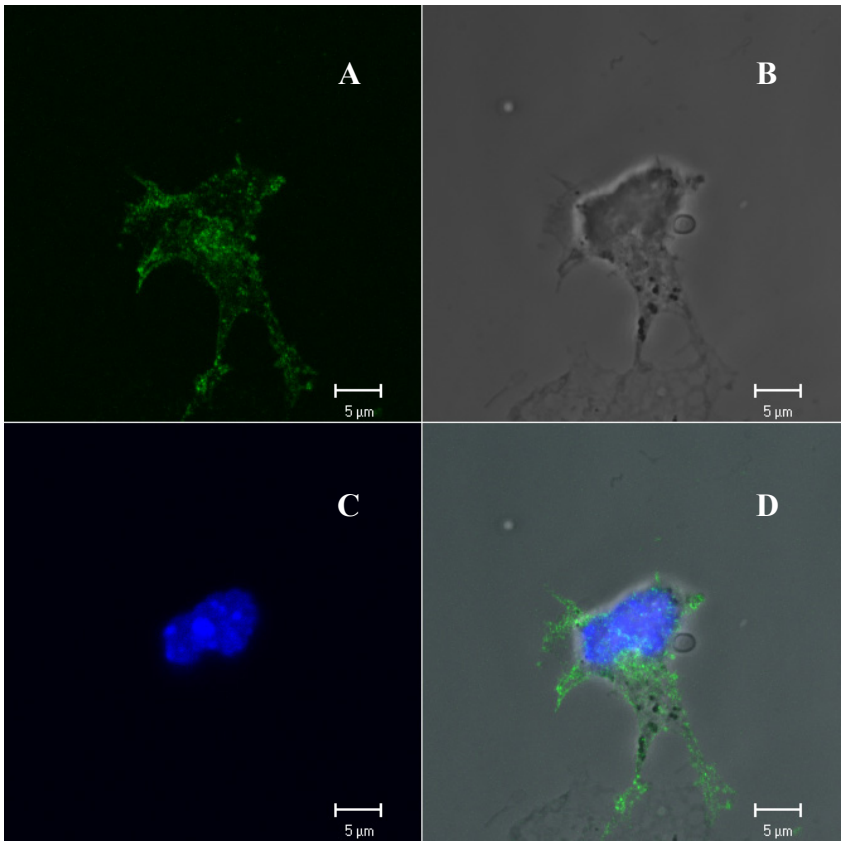

Figure 5.4 Images of immature esDC stained for the expression of MHC class II

EsDCs were seeded on to glass coverslips pre-treated with poly-L-lysine and incubated overnight before being washed, fixed with 1% paraformaldehyde, and permeabilised with saponin buffer and stained with IA-IE (MHC II) FITC conjugated antibody. In this picture we can notice that the cell is semi- adherent to the plastic. Indeed DCs usually strongly adhere to the culture dish once in the mature state. The cover-slip was then mounted on a glass slide using ProLong Gold containing DAPI. Panel A shows MHC class II marker (green), panel B reports the phase contrast image of the cells. Panel C reports in blue the DNA stained by DAPI, Panel D shows the combination of the previous panels.

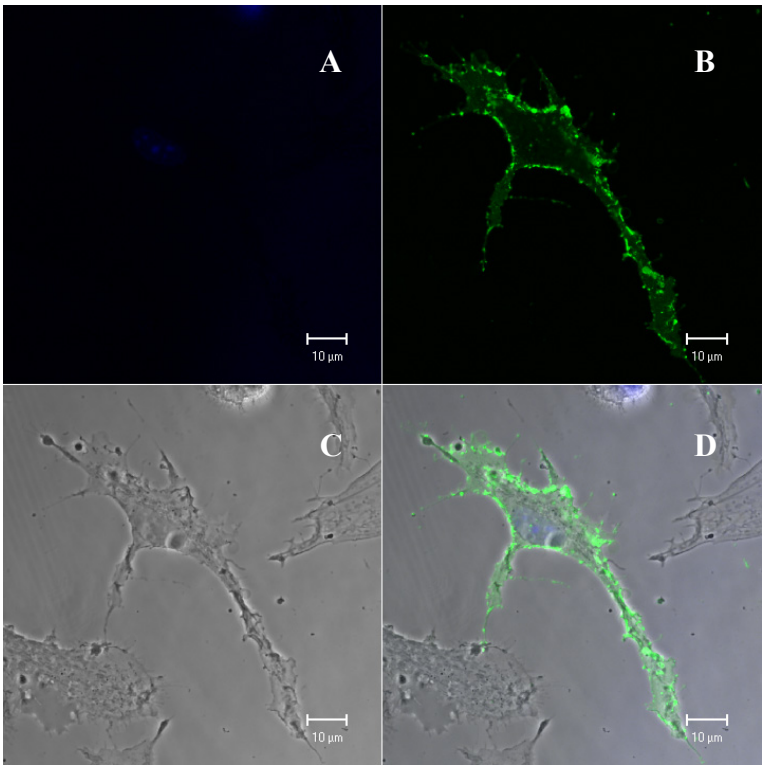

Figure 5.5 Confocal image of murine esDC after over night activation with TNFα and stained for MHC II

Mouse esDCs were seeded onto a 24 well plate containing a glass cover slip treated with poly-L-lysine and incubated overnight with GM-CFS and IL-3 free medium that contained TNFα. The cells were then fixed and stained for IA-IE (MHC II) marker (green). The cover-slip was then mounted on a glass slide using ProLong Gold containing DAPI (blue) which binds to DNA (panel A). Panel B reports the MHC class II marker (green), panel C reports the phase contrast image of the cells and panel D reports the combination of the previous panels. This is only one example of the images taken of esDC activated either with TNFα or LPS.

In order to verify if the candidate esDCs possessed the ability to degrade antigens, DQ-OVA was applied. DQ-OVA is a self-quenched conjugated protein that displays green fluorescence upon photolytic degradation. Antigen processing involves protein internalization, denaturation, proteolysis and the resulting peptides are associated with MHC class II to be presented on the cellular surface. Digested fragments of DQ-OVA accumulate in organelles at high enough concentration to be visualized by confocal microscopy (French *et al.*, 1997). This experiment proved that esDCs are able to process OVA, as a control protein antigen. In this experiment esDCs were seeded onto a cover-slip pre-treated with poly-L-Lysine, after overnight incubation, these were incubated for 2 hours with the labelled protein probe and then washed and incubated for 4 hours (after being treated with mitomycin C, which stops cell proliferation) to enable observation of the same cell over a long period of time. The cells were then mounted on a glass slide using ProLong Gold with DAPI to label DNA. Confocal images were taken and examples of these images can be found in Figure 5.6.

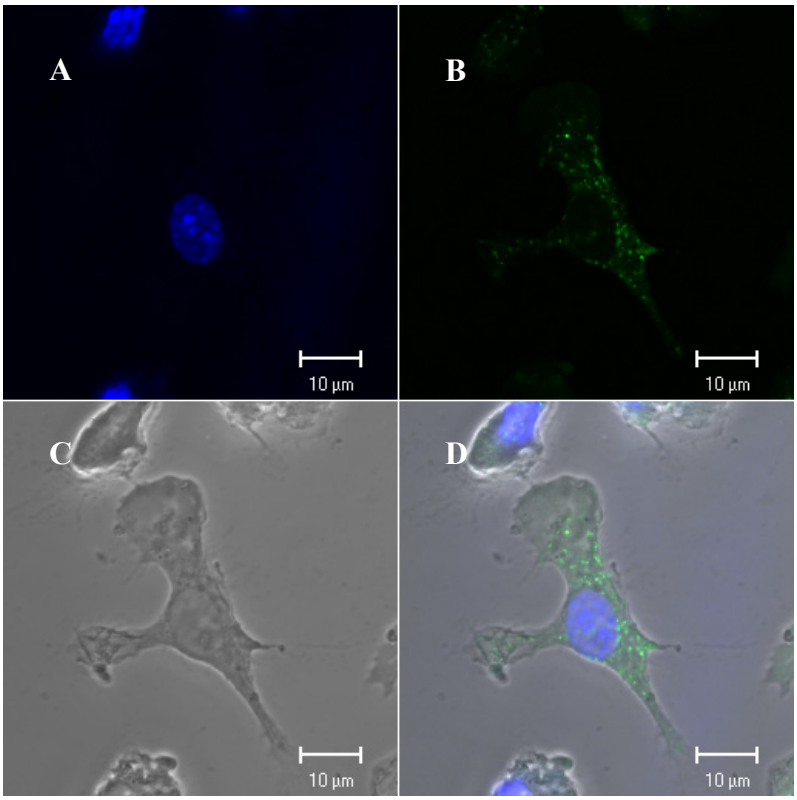

Figure 5.6 Confocal images of esDC incubated with DQ OVA

Confocal images of esDCs processing DQ-OVA. Panel A shows DAPI labeled nuclei; panel B shows processed DQ-OVA (green); panel C shows phase contrast image of the cell. Panel D shows the overlap of all these channels. The processed DQ-OVA can be noticed in green. Note also a large lamellipodium projecting from the cell.

5.2.4 Confocal investigation of esDCs infected with *S.* Typhimurium SL1344

Once a procedure for generating candidate esDCs had been developed the ability of these cells to interact with *S.* Typhimurium SL1344 was investigated. The interaction between esDCs and *S.* Typhimurium SL1344 was initially tracked using confocal imaging, following the initial bacterial contact and aspects of the subsequent internal vesicle trafficking. To this end murine esDCs were grown overnight on glass coverslips pre-treated with poly-L-lysine in medium free of GM-CSF and IL-3 and these were subsequently infected with *S.* Typhimurium SL1344(p1C/1), which expresses GFP. At 30 minutes post infection the esDCs were stained with an EEA-1 marker typically associated with the early endosome. At 3h similar esDCs exposed to *S.* Typhimurium SL1344 (p1C/1) were stained for the late lysosomal membrane glycoproteins (LMG) LAMP-1 and LAMP-2. Thses experiments were designed to investigate esDC-*Salmonella* interaction, potentially identifying the intracellular compartment occupied by *Salmonella*. Images representing this work can be found in Figure 5.7, 5.8 and 5.9.

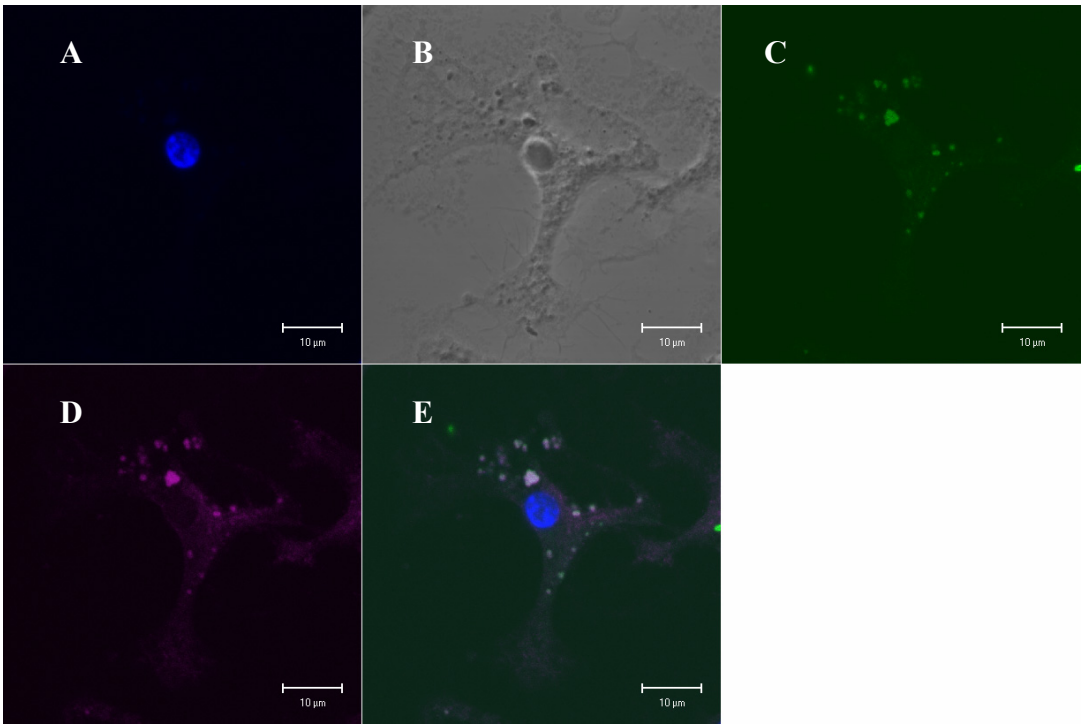

Figure 5.7 Confocal image of esDC infected with *S.* Typhimurium SL1344 (p1C/1)

Images of esDCs infected with *S.* Typhimurium SL1344(p1C/1) expressing GFP at 30 min post infection and stained with an antibody against EEA-1, a specific marker for early endosome revealed with a secondary antibody conjugated to APC Cy-7 fluorochrome. Panel A shows cell nuclei stained with DAPI (blue), panel B shows phase-contrast channel, panel C shows internalized bacteria (green), panel D shows EEA-1 marker (purple), panel E reports the alignment of the previous panels minus the light-contrast channel in order to improve the visualization of the colocalization. The images provide evidence for clear colocalization between the bacteria and the endosomal marker.

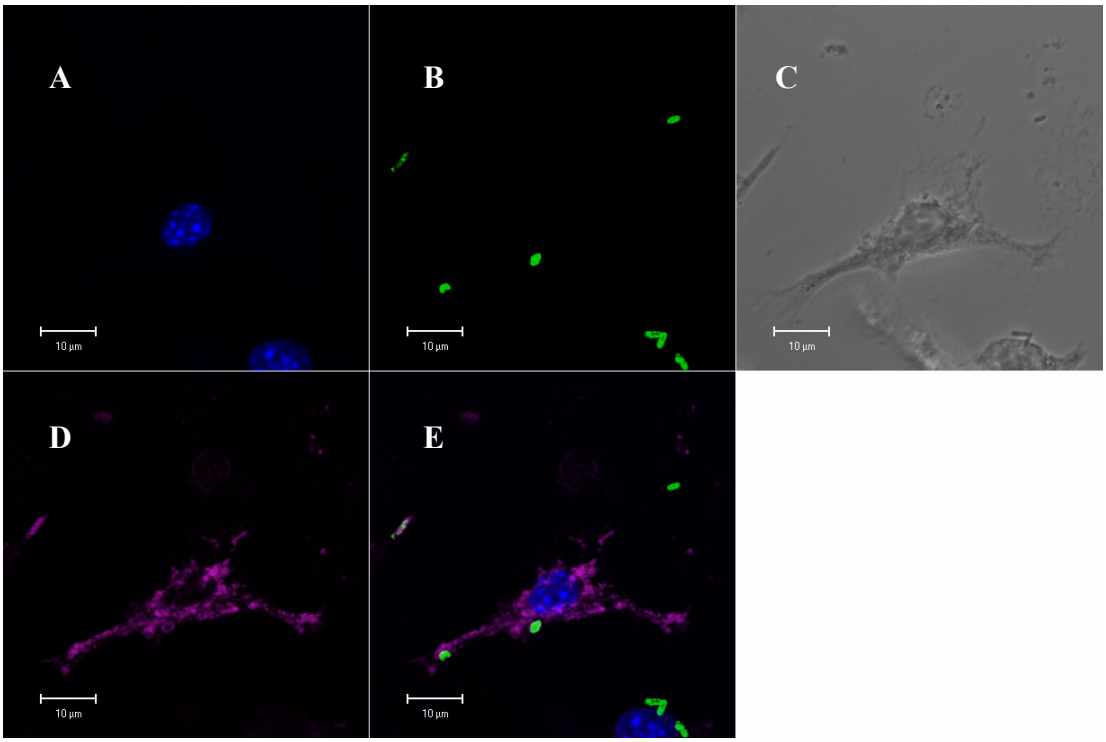

Figure 5.8 Confocal image of esDC incubated for 3h with *S.* Typhimurium SL1344 (p1C/1)

The images show in blue the nuclei stained by DAPI (panel A), green GFP-expressing *S.* Typhimurium SL1344(p1C/1) (panel B) and in purple LAMP-1 (panel D) is highlighted by a secondary antibody conjugated to APC-Cy7. Panel C reports the phase-contrast channel and panel E reports the combination of all the panels minus the light-contrast channel. This images indicates colocalization of the green bacteria and the LGP LAMP-1 at 3h infection time.

Murine esDCs were then examined by confocal microscopy for colocalization of *S.* Typhimurium with lysosome marker LAMP-2 at 3 hours post exposure. The esDCs were infected as described in M&M and fixed with 1% paraformaldehyde on ice for 20 min permeabilised with saponin buffer and stained with the appropriate primary and secondary antibodies. The result can be seen in Figure 5.9.

1

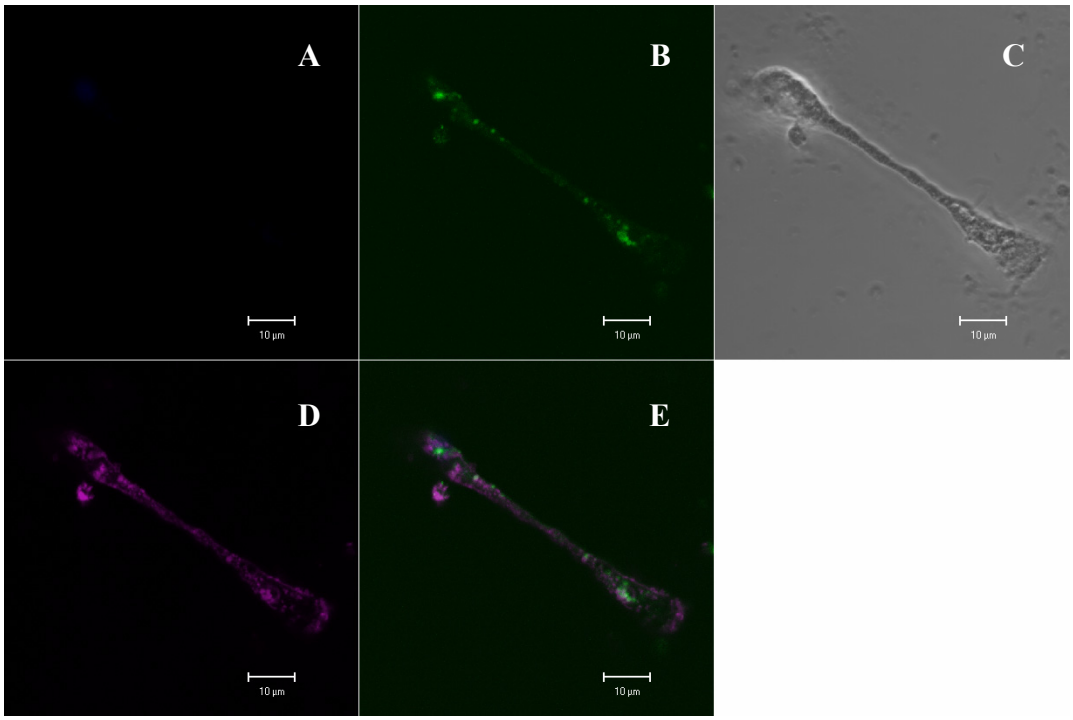

2

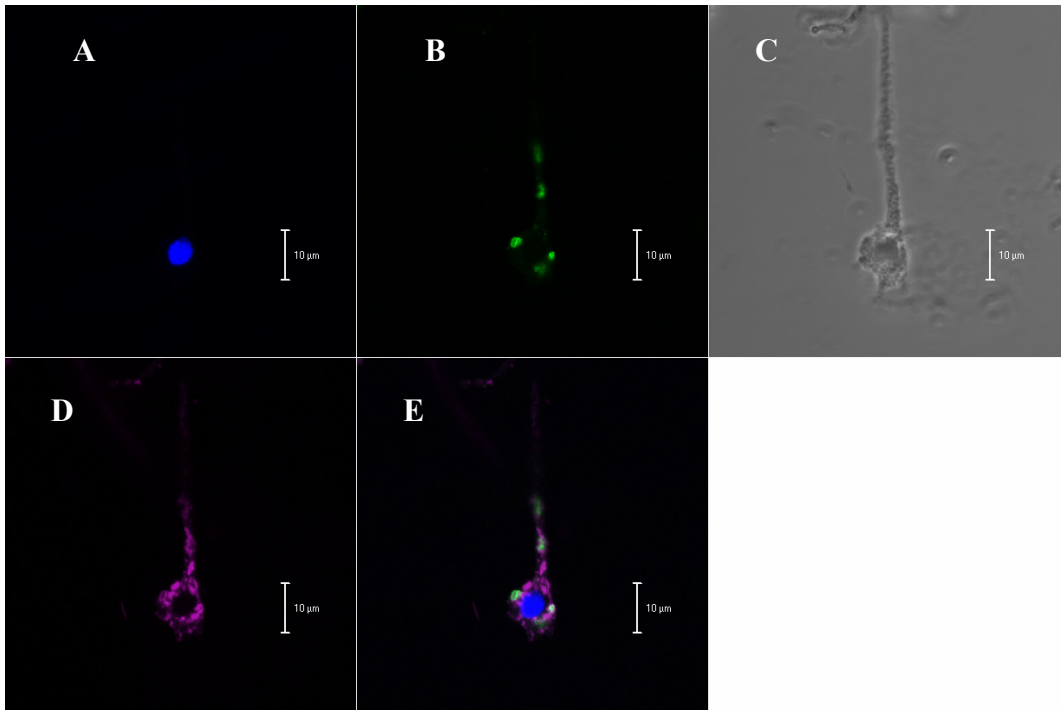

Figure 5.9 Confocal image of esDCs infected with *S.* Typhimurium SL1344 (p1C/1)

These images show esDCs infected with *S.* Typhimurium SL1344 (p1C/1) expressing GFP (green) panel B, at 3h post infection stained with an antibody against the LAMP-2 marker specific for late lysosomes and revealed by a secondary antibody conjugated with APC-Cy7 (purple), panel D. In blue are reported the nuclei labeled with DAPI, panel A. The phase-contrast channel images are reported in panel C. Panel E report the overlapping of all the channels for each image minus the light-contrast to simplify the

observation of colocalization. Here there is evidence for both colocalization and non-colocalization suggesting not all endosomes are fused to lysosomes. These observations agree with the contemporary literature on the interaction of terminally differentiated DCs with *S*. Typhimurium, where researchers have conflicting opinions. See Discussion.

5.2.5 Electron microscopy characterization of esDCs

Murine esDCs were investigated for morphology changes and general integrity using electron microscopy. These images were taken using AB2.2 ES cells and derived esDCs with the help of Dave Goulding, the electron microscope officer at the WTSI (Figure 5.10). The EM observations highlighted the differencies in morphology between the original murine ES cells and the derived esDC, in particular the presence of membrane protrusion, ER expansion and the higher number of mitocondria in esDC. These traites are characteristic of antigen presenting cells, whereas ES cells are characterized by a large nuclei and small cytosol content (Figure 5.10, image 1). Murine AB2.2 ES and esDCs were observed using transmission electron microscopy at 1 hour post exposure to *S.* Typhimurium SL1344. In both cell types the *Salmonella* associated vacuole can be seeen in some cases adjacent to or fused with lysosomal vacuoles (Figure 5.10, black arrows).

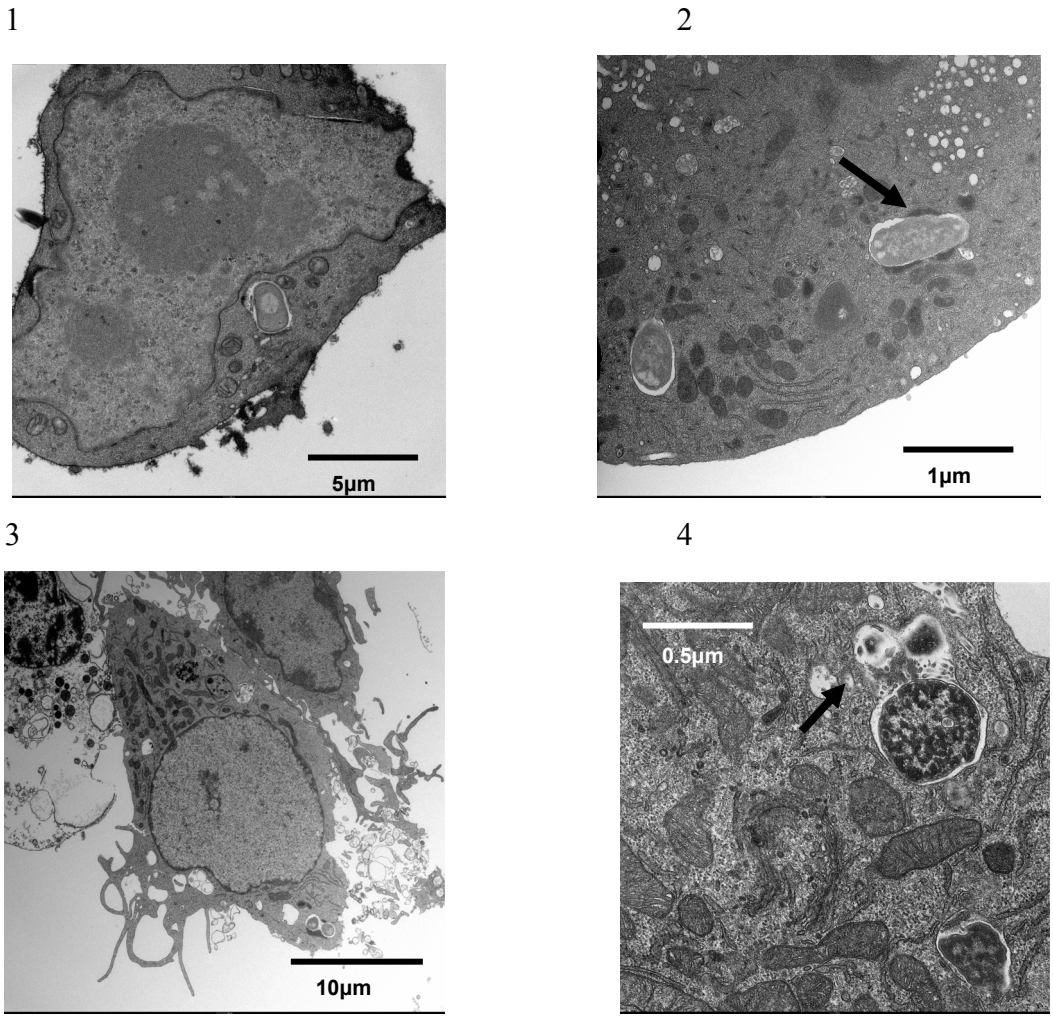

Figure 5.10 Transmission electron microscopic images of undifferentiated murine ES cells AB2.2 and derived esDC during infection with *S.* Typhimurium SL1344

Panel 1 shows a whole AB2.2 murine ES cells infected by *S.* Typhimurium SL1344. Panel 2 *S.* Typhimurium SL1344 bacteria can be seen inside the SCV apparently under attack by lysosomes. Panels 3 and 4 show the morphology of a whole esDC and a *S.* Typhimurium bacterium inside the cell. The balck arrows indicate potential lysosomal vacuole fusion with the SCV.

5.2.6 Functional assays on esDCs

5.2.6.1 Cytokine production by esDCs

In order to investigate the functional activity of esDCs, the expression of cytokines was measured using a Cytometric Bead Array (CBA) assay from Becton Dickinson Biosciences as described in M&M. A standard kit, normally used for mouse inflammation analysis monitored the production of Interferon γ (IFNγ), Interleukin-10 (IL-10), Interleukin-12p70 (IL-12p70), Interleukin-6 (IL-6), Monocyte Chemo-attractant Protein-1 (MCP-1) and TNF. Experiments monitored potential cytokine expression during *S.* Typhimurium SL1344 invasion of murine AB2.2 ES cells and derived esDCs. The results are shown in Table 5.2. Cytokine production after incubation of esDCs with LPS, OVA or TNFα was also assessed (Table 5.3).

Table 5.2 The levels in pg/ml of cytokines produced by AB2.2 murine ES cells and esDCs infected and uninfected with *S.* Typhimurium SL1344.

The amount of cytokine produced by AB2.2 murine ES cells and esDC alone or during infection with *S.* Typhimurium are reported in pg/ml. Each value represents the mean of at least two measurements ± 1 SD. The detection limits of the assay are 2.5pg/ml for IFNγ, 17.5pg/ml for IL-10, 10.7 pg/ml for IL-12p70, 5pg/ml for IL-6, 52.5pg/ml for MCP-1 and 7.3pg/ml for TNF. ND = Not determined (below the detection limit).

Cytokines pg/ml	AB2.2 no bacteria	AB2.2 with SL1344 30minutes	AB2.2 with SL1344 2hours	AB2.2 with SL1344 4hours	esDC no bacteria	esDC with SL1344 30minutes	esDC with SL1344 2hours	esDC with SL1344 4hours
IFNγ	ND	ND	ND	ND	ND	ND	ND	ND
IL-10	ND	ND	ND	ND	ND	ND	33±21	56±35
IL-12p70	ND	ND	ND	ND	ND	ND	ND	ND
IL-6	ND	ND	ND	ND	ND	5.5±1.4	30.5±0.7	400.5±108
MCP	ND	ND	ND	ND	108±117	138±80	181±54	339±0
TNF	ND	ND	ND	ND	26±24	134.5±67	1673±287	3538±1254

Table 5.3 Cytokine production by esDCs and BMDCs activated with *S.* Typhimurium LPS 10µg/ml, OVA protein 10µg/ml or TNFα 5000 WHOSU/ml

The DCs were seeded in 96 well plates at $1x10^5$ cells per well and incubated overnight with LPS, OVA or TNFα. The supernatants were collected and frozen at -20ºC until analyzed by CBA. EsDC and BMDC were each maintained in their own medium. Results obtained with TNFα are not reported in this table. (See below). The detection limits of the assay are 5pg/ml for IL-6, 17.5pg/ml for IL-10, 52.5pg/ml for MCP-1, 2.5pg/ml for IFNγ, 7.3pg/ml for TNFα and 10.7 pg/ml for IL-12p70. ND = Not determined (below the detection limit).

Cytokine pg/ml	esDCs alone	esDC with OVA 24h	esDC with LPS 24h	BMDC alone	BMDC with OVA 24h	BMDC with LPS 24h
IFNγ	ND	ND	ND	ND	ND	35
IL-10	ND	ND	575	ND	ND	ND
IL-12p70	ND	ND	ND	ND	ND	215
IL-6	15	643	13262	ND	166	10541
MCP	3607	6205	9709	102	175	1162
TNF	545	1356	6005	53	212	7068

Table 5.4 Cytokine production by esDCs and BMDCs during antigen presentation assay

The same supernatants derived from the antigen presentation assay tested for IL-2 concentration (Table 5.5) were also tested for cytokine production. The detection limits of the assay are 5pg/ml for IL-6, 17.5pg/ml for IL-10, 52.5pg/ml for MCP-1, 2.5pg/ml for IFNγ, 7.3pg/ml for TNFα and 10.7 pg/ml for IL-12p70. ND = Not determined (below the detection limit).

Cytokine pg/ml	BMDC	BMDC with T cells	BMDC with T cells and OVA 24h	BMDC with T cells and OVA 48h	BMDC with T cells and TNFα 24h	BMDC with T cells and TNFα 48h	T cells with ConA
IFNγ	ND	ND	ND	ND	ND	ND	ND
IL-10	ND	ND	ND	ND	20	23	97
IL-12p70	ND	ND	ND	ND	ND	ND	ND
IL-6	98	42	1243	1927	206	167	ND
MCP	1558	1745	2176	2490	2525	1909	ND
TNF	1973	892	3794	3875	9839	8805	145
Cytokine pg/ml	**esDC**	**esDC with T cells**	**esDC with T cells and OVA 24h**	**esDC with T cells and OVA 48h**	**esDC with T cells and TNFα 24h**	**esDC with T cells and TNFα 48h**	**T cells with ConA**
IFNγ	ND	ND	ND	ND	ND	ND	ND
IL-10	ND	21	ND	ND	ND	ND	62
IL-12p70	ND	ND	ND	ND	ND	ND	ND
IL-6	17	9	218	156	29	18	ND
MCP	1339	1638	4009	1834	1825	862	ND
TNF	1264	348	1099	776	6621	5220	147

5.2.6.2 Antigen presentation assay

In order to test the ability of esDC to process and present antigens to the allogenic T cell line MF2.2d9, antigen presentation assays were performed and IL-2 production measured with a CBA kit as described in M&M. The same supernatants were also used in standard CBA assays to measure IFNγ, IL-10, IL-12p70, IL-6, MCP and TNF concentrations (Table 5.4). The IL-2 concentrations reported here is an example from a typical assay. The two types of dendritic cells were treated on the same day and the same T cell stock was applied. The data can be found in Table 5.5

Table 5.5 IL-2 production by T cells activated during antigen presentation assays involving BMDCs and esDCs

The MF2.2d9 T cells were incubated for 24 and 48h with 12 day old BMDCs and 14 day old esDCs at a 1:5 ratio with OVA 10µg/ml. TNFα 5000 WHOSU/ml was also included in this assay as negative control. The culture supernatant was collected and the concentration of IL-2 was tested using a CBA Flex Set from BD Biosciences. ND = Not determined (below the detection limit of 2pg/ml).

Sample	BMDC	BMDC with T cells	BMDC with T cells and OVA 24h	BMDC with T cells and OVA 48h	BMDC with T cells and TNF 24h	BMDC with T cells and TNF 48h	T cells with ConA in IMDM
IL-2 pg/ml	ND	11	77	85	3	5	147
Sample	**esDC**	**esDC with T cells**	**esDC with T cells and OVA 24h**	**esDC with T cells and OVA 48h**	**esDC with T cells and TNFα 24h**	**esDC with T cells and TNFα 48h**	**T cells with ConA in DMEM**
IL-2 pg/ml	ND	3	43	47	5	8	101

5.3 Discussion

This chapter reports a summary of the results of investigations on the properties of murine AB2.2 ES cells differentiated *in vitro* into APCs which resemble DCs (esDCs). To this end a version of the protocol published by Dr. Fairchild from the Sir William Dunn School of Pathology, Oxford (Fairchild *et al.*, 2000; Fairchild *et al.*, 2003) was exploited. In 2003 a second group reported the differentiation of DCs from mouse ES cells using embryoid body formation and co-culture with an OP9 feeder cell layer (Senju *et al.*, 2003). The authors of these papers recognized the potential importance of these *in vitro* methods combined with the ability of ES cells to be genetically engineered. Indeed, an ever increasing number of different gene-trap ES libraries are already available [www.genetrap.org].

DCs are the most potent APCs present in the body and they are considered to be the connection between the innate and the adaptive immune responses. In fact DCs are the cells responsible for the priming of naïve T cells in an antigen-specific manner. Immature DCs exhibit endocytic activity that occurs via several pathways: fluid phase pinocytosis, including macropinocytosis; receptor-mediated uptake via Fc receptors and the action of lectin receptors, such as the macrophage mannose receptor (MMR). In addition DCs are able to phagocytose microbes and dying cells. The capacity of DCs to process dying cells has drawn enormous attention since it may lie at the heart of many challenging problems in medicine including transplant rejection, self-tolerance, immunity to viral and bacteria-infected cells and tumor immunity. This highlights the importance of these cells in the body homeostasis.

Flow cytometry results

EsDC were initially characterized for their surface marker expression by flow cytometric assays. They were compared to undifferentiated ES cells and BMDCs. Undifferentiated ES cells do not express markers normally distinctly described as specific immune cell markers but they do express significant levels of cytokines (Guo *et al.*, 2006). Examples of markers specific for leukocyte cells and a few specific for DCs include CD11b, CD11c, H-2K, I-A/I-E, CD40, CD44, CD45, CD54, CD80, CD86, DC-SIGN, Ly-6C and CD-205. The expression of these markers by murine AB2.2 ES cells,

BMDCs and esDCs in the immature state and in the mature state obtained following treatment with LPS, OVA protein or TNFα was assessed. As expected the murine AB2.2 ES cells did not express the majority of these markers. However, after growth under the conditions reported here they expressed detectable levels of CD40, CD54, and F4/80 markers in addition to DC-SIGN (Table 5.1). These results do not match with previously published information on ES cells. However, it is known that ES cells do not produce detectable amounts of MHC class II and only a small amount of MHC class I (Magliocca *et al.*, 2006; Menendez *et al.*, 2005); consistent with the results reported. Reports indicate that ES cells should not normally produce CD40, B7-1 and B7-2 (Tartour & Kadereit, 2006). However some of these markers have been reported on myeloid progenitor cells (Odegaard *et al.*, 2007). Also, this may mean that the Sv/129 ES cells described here have the right qualities to differentiate into leukocytes. Murine AB2.2 ES cells were first maintained on a feeder cells layer before being cultured for two passages on medium containing LIF in order to obtain a pure culture. Subsequently, the cells were cultured in suspension on a bacteriological Petri dish with medium free of LIF in order to produce EBs. Fourteen day old EBs were then seeded onto a culture dish with medium containing GM-CSF and IL-3 and esDCs were harvested in the following 7 to 30 days. The esDC so obtained were theoretically in the immature state..

During maturation experiments esDCs were exposed overnight to *S.* Typhimurium LPS at 10μg/ml and an increase in the expression of CD11b, CD11c, CD4, CD40, CD54, CD8, CD80 and 86, DC-SIGN, H-2K, TLR2 and TLR4 was detected by flow cytometric analysis (Table 5.1). After overnight incubation with TNFα esDCs displayed enhanced the expression of CD11b, CD11c and IA-IE, whereas after incubation with OVA protein, esDCs showed an increased expression of the markers CD80 and TLR4. All together a stronger enhanced expression of activated markers was observed after overnight incubation with *S.* Typhimurium LPS. However BMDCs showed even stronger expression of activation markers. All the DC lines were positive for a DC selectively expressed lectin called DC-specific intercellular adhesion molecule 3-grabbing non-integrin (DC-SIGN), which binds to the intracellular adhesion molecule (ICAM)-3 on resting T cells and enhances the DC-T cell interaction. This indicated that esDCs could harbour the potential to initiate specific immune responses from resting T cells (Soilleux, 2003).

Microscopic observations

The expression of MHC class II was not clearly demostrated by flow cytometric analysis. It is possible that the FITC fluorochrome chosen to reveal this marker was too weak to assess its expression. Consequently, confocal examination of the expression of MHC class II molecules by esDCs was carried out. Observations at the confocal microscope reported in Figures 5.4 and 5.5 confirm that some candidate esDCs expressed detectable MHC class II markers but other cells did not, so a non-uniformity in the maturation of esDC can be seen although all the cells show the characteristic morphology of DCs. The ability of esDCs to process DQ-OVA was also investigated by confocal microscopy (Figure 5.6). It was possible to observe that all the cells contained green-OVA at 4 hours incubation. Unfortunately, a clear observation of the antigen presentation on the cell surface at 24 hours post incubation was not possible since it was impossible to distinguish between the internal OVA and the surface OVA. It is also likely that only an accumulation of DQ-OVA can be detected, like in lysosome compartments, but the surface exposure of processed peptides cannot.

A number of reports have indicated that *S.* Typhimurium is unable to replicate efficiently inside DCs (Jones & Falkow, 1996; Niedergang *et al.*, 2000). This may be a deliberate act by the bacteria that is possibly connected to the ability of *S.* Typhimurium to avoid the MHC class I and II compartments in order to survive inside the host cell. Indeed it is recognized that the TIIISS harbored by SPI-2 alters lysosome trafficking in order to avoid phagosome-lysosome fusion (Abrahams & Hensel, 2006; Uchiya *et al.*, 1999).

Interestingly, there is an on going debate in the scientific community regarding whether *S.* Typhimurium colocalizes inside DCs with LAMP-1 and LAMP-2 lysosomes markers. Garcia-Del Portillo and coworkers reported only 5% of the internalized bacteria were colocalized with the lysosomal membrane glycoprotein (LPGs) LAMP-1, and no colocalization was detected with other LGP markers such as LAMP-2 during infection of murine splenic DC line CB1 (Garcia-Del Portillo *et al.*, 2000). However other researchers reported strong evidence of the colocalization of wild type *S.* Typhimurium with the LAMP-1 marker 90 min after infection and clear colocalization with MHC class II (Jantsch *et al.*, 2003; Petrovska *et al.*, 2004). In this study, colocalization was detected between *S.* Typhimurium and the early endosome marker

EEA-1 and with LAMP-1 in esDCs (Figure 5.7 and 5.8). However, confocal observation detected both colocalization and non-colocalization with LAMP-2 marker in this study, suggesting there may be a mixed pattern within cells (Figure 5.9.). This confirms the need to further investigate the vesicular pathway used by *S.* Typhimurium inside DCs.

In this chapter electron microscopic investigations were also described to confirm the difference in morphology between the original murine AB2.2 ES cells and the derived esDCs. Expanded ER and Golgi apparatus and increased number of mitochondria were consistently observed in esDCs. Also numerous lysosomes vacuoles were detected. Moreover, the multi-laminar structures, typical of 'empty' MHC class II compartment, or *Salmonella* containing vacuoles were also identified lately. The latter structures, SCV with multilaminar membrane, were previously observed in only 5% of the SCV containing wild-type *Salmonella*, after 20h of infection (Garcia-Del Portillo *et al.*, 2000).

Functional assay results

Finally, esDCs were further analyzed using functional immune assays. The ability of esDCs to produce cytokines during *S.* Typhimurium infection was measured by CBA assays and their level of secretion was compared to the production of cytokine by the original murine AB2.2 ES cells. The production of cytokine by murine ES cells is not surprising and in fact it had been described previously that ES cells are regulated by cytokines (Kristensen *et al.*, 2005). Murine ES cells were described to produce, in the presence of LIF, cytokine including IL-10, MCP-1 and TNFα (Guo *et al.*, 2006) but in the present study they were all below detection limits. Immature DCs usually do not produce high levels of cytokine (Lutz & Schuler, 2002). In this study esDC supernatant was tested after 24 hours incubation for cytokine content and revealed the production of IL-6 and MCP-1. The other cytokine levels were below detection limits (Table 5.2).

Maturation of DCs is a process that involves the down-regulation of the antigen capturing capacity and up-regulation of MHC molecule synthesis and enhancement of the intracellular trafficking (Wick, 2002). In order to prove that esDCs are real functioning APCs, their ability to process protein antigen and activate T cells was tested together with cytokine production. The cytokines TNF, IL-12p70 and IFNγ were

measured since they play an important role in the survival of the host during *Salmonella* infection (Mittrucker & Kaufmann, 2000), and the ability of DCs to produce these cytokines upon encountering this bacteria has been demonstrated. Most reports describe the production of IL12-p40 and little production of the bioactive form IL12-p70 (Svensson *et al.*, 2000; Yrlid & Wick, 2002). One hypothesis to justify this observation could be the lack of accessory signals or cytokines from the surroundings to sustain and enhance the DC response (Niedergang *et al.*, 2000; Schulz *et al.*, 2000). Also, IFNγ secretion by infected and mature DCs was investigated. IFNγ is a cytokine important in controlling many bacterial infections. The capacity of DCs to produce IFNγ is controlled and dependent on IL-12 production (Fukao *et al.*, 2000; Hochrein *et al.*, 2001; Stober *et al.*, 2001). In this study, the production of IL-12p70 by esDCs was not observed during bacterial infection or after overnight incubation with LPS, OVA or TNFα. However, a substantial production of IL-12p70 was observed for BMDCs coincubated with *S.* Typhimurium LPS. The same sample contained a significant concentration of IFNγ, confirming the literature cited (Table 5.3).

The level of IL-10 production was also investigated. IL-10 is an anti-inflammatory cytokine involved in the immune response to bacteria, down regulating the inflammation stimulus that can damage the tissues and help infection spread. Although previous studies reported that DCs can prime T cells to produce IL-10, the production of IL-10 by DCs infected by *S.* Typhimurium is not always detected (Marriott *et al.*, 1999). EsDCs produced detectable amounts of IL-10 during infection with *S.* Typhimurium at 2 hours and 4 hours (Table 5.2) incubation time and after overnight incubation with LPS (Table 5.3), whereas it was not possible to detect significant amount of IL-10 produced by BMDCs (Table 5.3). It should be noted that the production of even low amounts of IL-10 can reduce remarkably the release of IL-12p40 (Siegemund *et al.*, 2007), which could explain the lack of IL-12 production in the experiments here reported.

Additionally in this study the pro-inflammatory cytokines IL-6 and TNF were investigated. The data here reported revealed that esDCs and BMDCs produce IL-6 in the presence of *S.* Typhimurium, after activation with *Salmonella* LPS and OVA (probably due to LPS contamination) (Table 5.3) and after incubation with TNFα (Table 5.4). The production of IL-6 during the *in vitro* infection of DCs was previously observed (Marriott *et al.*, 1999). Also the production of TNFα was detected during

esDCs and BMDCs infection with *S.* Typhimurium (Table 5.2) and during activation with LPS or OVA (Table 5.3). The production of TNFα by DCs during infection with *Salmonella* and incubation with LPS was described previously (Siegemund *et al.*, 2007). These cytokines have been reported to be important for DC maturation (Park *et al.*, 2004; Sundquist & Wick, 2005).

DCs can produce MCP-1 of which secretion is TLR mediated. This cytokine was produced by esDCs infected with *S.* Typhimurium SL1344 (Table 5.2) and BMDCs incubated with *Salmonella* LPS (Table 5.3). The production of MCP-1 probably is related to the binding of TLR ligands, one of which is LPS, and this is a MyD88 dependent process. Also the contribution of MAPK and NF-κB signaling to TLR-mediated MCP-1 secretion was reported previously. Moreover, using IFNαβR$^{-/-}$ knock-out mice it was observed that MCP-1 expression by TLR is dependent on the production of type–I interferon, in our assay we tested for type-II IFN, γ (Vivekanandhana & Klinmana, 2007). This may be the reason why IFNγ wasn't detected in the experiments here reported. Moreover the production of MCP-1 by esDCs thought to be in the immature state may be a sign that these DCs are really in the mature state (Table 5.2).

Perhaps the critical data presented here is that esDCs were able to process the protein antigen OVA, express the peptide antigen on their surface and activate T cells CD4+ to produce IL-2 (Table 5.5). This activation also absolutely requires the co-expression of co-stimulatory signals like CD80 and CD86 by the same APC (Greenwald *et al.*, 2005). This is the best proof that esDCs are real APC.

In conclusion, this chapter described the differentiation and characterization of APC deriving from *in vitro* differentiation of murine ES cells. In the next chapter these cells will be investigated during *S.* Typhimurium infection, applying microarray technology to investigate their biological response to bacterial infection. This technique might help also to clarify the doubts about the real nature of esDCs.